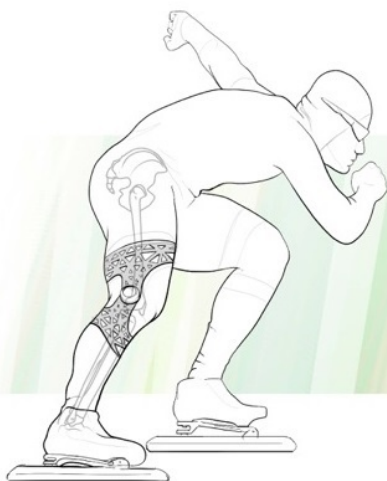


Bachelor Thesis

GonioTrainer

B. Bosma ,
M.C. Scoop ,

4240898
4203615



Bachelor Thesis

GonioTrainer

by

B. Bosma ,
M.C. Scoop ,

4240898
4203615

to obtain the degree of Bachelor of Science
at the Delft University of Technology,

Student:	B. Bosma	4240898
	M.C. Scoop	4203615
Project duration:	April 20, 2015 – June 22, 2015	
Thesis committee:	Dr. ir. W. A. Serdijn,	TU Delft
	Dr. ing. I. E. Lager,	TU Delft
	Ing. J. Bastemeijer,	TU Delft
	MSc. O. den Braver,	O'Sports

This thesis is confidential and cannot be made public until December 31, 2018.

An electronic version of this thesis is available at <http://repository.tudelft.nl/>.

Preface

This bachelor thesis has been written for the completion of the Bachelor of Science study Electrical Engineering provided by Delft University of Technology. This thesis was written by Bas Bosma and Mitchell Scoop. As a subgroup of a group of six they were responsible for the power supply of the GonioTrainer and for the realtime feedback. This project was provided by Otto Den Braver from the company O'sports. The project was carried out under Prof. Dr. Kofi Makinwa. Furthermore we are thankful to Diederik Van Steen for sharing his previous versions, visions and ideas, and Jeroen Bastenmeijer for the continuous guidance throughout the entire project.

*Bas Bosma
Mitchell Scoop
Delft, juni 2015*

Abstract

Increasing physical performance in this day and age is aided by technology. The GonioTrainer is a device which will measure a joint angle and give the user visual feedback on a smartphone, real time haptic feedback using a feedback module, and elaborate visual feedback on a computer or tablet after a session of usage. This device will consist out of two modules, the goniometer, which is the module that will perform all measurements, and the feedback module, which will provide the haptic feedback.

The GonioTrainer will measure the joint angle with a frequency of 100Hz . An algorithm will make the decision whether haptic feedback should be given or not. This algorithm will not be implemented by the project group and will thus not be reported in this thesis. However, the algorithm for determining *when* the haptic feedback should be given will be implemented, using a peak detection algorithm from data received by an inertial measurement unit. The time window between deciding when haptic feedback should be given and actually receiving said feedback will be no more than 50ms .

In this thesis the power supply choices and corresponding circuitry, for both the goniometer and feedback module will be implemented, documented and analysed. A prototype for the feedback module will be designed and implemented.

Power consumption for a time period of 3 hours was done which concluded a rechargeable battery with a capacity of 240.1mAh will be needed for the goniometer, and a battery with a capacity of 127.22mAh for the feedback module. Due to the dimensions of both modules, a battery with a Lithium-Ion Polymer chemistry was chosen. These batteries will need recharging. A suitable charger was sought and found. In order to indicate whether a battery is nearly empty, a battery fuel gauge was implemented so the remaining active relative capacity could easily be displayed.

The feedback module was implemented using a 9mm eccentric rotating mass DC motor. As a method to control the motor, a motordriver was chosen. Both the gauge and the motordriver have an I²C interface.

Contents

1	Introduction	1
2	Problem Definition	2
2.1	Current Product	2
2.2	Demands	2
2.2.1	The use	2
2.2.2	Design specifications	3
2.3	The Task/Objective	5
3	System Concept	6
3.1	System Architecture	6
3.1.1	Connection Architecture	6
3.1.2	Power management	7
3.1.3	Sensors	8
3.1.4	Prototyping	8
3.2	Power Supply	9
3.2.1	Power consumption	9
3.2.2	Review batteries	11
3.2.3	Cylindrical cell	12
3.2.4	Button cell	12
3.2.5	Prismatic cell	12
3.2.6	Pouch cell	13
3.2.7	Conclusion	13
3.3	Battery Protection	13
3.4	Battery Charging	13
3.4.1	Linear chargers	14
3.4.2	Switching chargers	14
3.4.3	Pulse chargers	15
3.4.4	USB compatibility	15
3.4.5	Power path management	15
3.5	Low Battery Indication	15
3.5.1	Coulomb counter	16
3.5.2	Dynamic voltage-based fuel gauge	17
3.5.3	ModelGauge m3	17
3.6	DC-DC Converter	17
3.6.1	Linear regulator	17
3.6.2	Switching regulator	17
3.6.3	Charge pump	18
3.7	Motor Driving	18
3.7.1	MOSFET with PWM	19
3.7.2	Driver IC	19
4	Implementation	20
4.1	nRF51822 Development Board	20
4.2	Battery	20
4.3	Battery Protection	21
4.4	Battery Charger	22
4.4.1	Power Path Management	23

4.5	Buck-Boost DC/DC converter	24
4.6	Battery Gauge	26
4.7	Vibration Motor	27
4.7.1	ERM motor	27
4.7.2	Motor driver	27
4.7.3	Adjustable settings	28
4.8	Final Design	29
5	Results	30
5.1	Battery Protection, Battery Charging, Power Path Management & Battery Gauge	30
5.2	Motor driver	31
5.3	Feedback control via smartphone	32
5.4	Weight and size	32
5.5	Pricing	32
6	Discussion	34
6.1	Use of buck converter	34
6.2	Driver directly connected to the battery	34
7	Ethics	35
7.1	Consequentialism	35
7.2	Virtue Ethics	35
7.3	Deontological ethics	35
7.4	Philosophy of dialogue	36
7.5	Conclusion	36
8	Conclusion	37
A	RedBearlab nRF51822	38
A.1	Board pinout	38
B	DRV2605L	39
B.1	Block diagram	39
B.2	Output-input graph	40
B.3	Pico Vibe performance graph	40
C	Total Design	41
C.1	Schematic.	41
	Bibliography	42

Introduction

When it comes to sports, the technique of an athlete is of great importance for the performance. One aspect that plays a role in many sports, is the angle of a joint, e.g. in ice skating the angle of the knee is important for reducing the frontal area, which will decrease the air drag. By being able to measure a specific joint angle, unique insights and feedback can be given to athletes and coaches. By analysing the measured data, a very specific training program can be established. This will help increase performance very effectively.

Coaches are usually the ones that have to give feedback about the angles that are known for improving performance and a lot of other aspects. Tracking multiple aspects of an athlete's technique at once can be difficult and inaccurate. This limits the effectiveness of coaches during one observation. Technology can be an aid for coaches and athletes alike.

This is where the device created for this thesis comes into play. Because a specific joint angle can provide valuable data, this device will measure the joint angle of the joint it is attached to. This data will be evaluated to judge whether the measured angle is the optimal angle; the optimal angle being a user defined angle. If it was not, a signal will be sent to the feedback module, which will give haptic feedback in the form of a vibration to the athlete. All of this should be done in real time and will allow the user to feel whether his/her joint angle was right or not and make corresponding adjustments in their subsequent movements. This is why this form of haptic feedback implemented in this product will be referred to as *direct feedback*. This device will need power, provided by a battery. Batteries are no equipment to mistreat, therefore the circuitry surrounding a battery should involve safety measures. Moreover, an athlete could be performing an action which involves a high chance of tumbling or slipping. When he/she does slip and lands on the GonioTrainer, it is an absolute requirement for the battery to not cause the user harm. This training device will be called the *GonioTrainer*, for Gonio means angle in Greek.

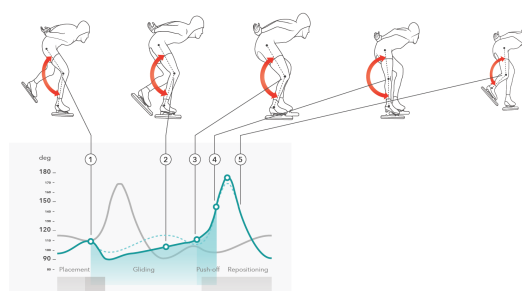


Figure 1.1: An example of how the device will register a joint angle.

In this thesis the design process of a part of the system proposed by the company O'sports, will be discussed. The proposed system will have a couple of sensors which will provide the necessary data for the implementation of a feedback algorithm. The thesis will start off with a deeper definition of the problem and will clarify the question of what is already implemented and what needs to be done. The implementation and results will then be presented, followed by a discussion and possible recommendations. The thesis will then end with short chapter on the ethical aspect of the matter and a conclusion.

2

Problem Definition

2.1. Current Product

The client, O'sports, is looking to develop a device that can measure a joint angle in order to send feedback to the user. The idea was first developed for ice skating, but now the development is targeted at multiple sports. The first version consisted of a device measuring the angle and storing this data. This was done using an RFDuino. This data was analysed in MatLab after which feedback could be given. Thereafter a feedback module was added. This was done to inform the user about his/her joint angle in real time. The haptic feedback was experienced differently by different users since some users are more sensitive to the haptic motion than others. Furthermore the moment of giving feedback proved to be important for an athlete to process the feedback; if feedback is constantly given at a different phase of each successive movement, athletes found it difficult to understand the feedback. Currently the product does not measure the phase consistently. Giving the feedback at the right time has thus far not been successful. Each user has a different stance and movement attributes, so finding the right parameters so that each user could use this device for direct feedback is very complex.

2.2. Demands

The current product needs to be upgraded. The system consists of a separate measurement module containing all the sensors with the ability to store data, which will be referred to as the *goniometer* from now on, and a separate feedback module. However, real-time feedback for the user must be added without the loss of the current functions. The target audience are athletes who stand to gain something by accurately measuring a joint angle. For professional athletes it can supplement the coach and for non-professional athletes it can fulfil the role of a (virtual) coach.

2.2.1. The use

The GonioTrainer will generally be used 4 times a week, in both matches and trainings. However, during matches, no smartphone or feedback module will be present. During trainings the user will have the smartphone, goniometer and the feedback module. A training will take up to 1.5 hours and could thus be used up to four times for 1.5 hours per week.

The goniometer will be attached to the joint of which the user is interested in. Attachment will be done by two elastic bands, one around the upper limb of said joint, and one around the lower limb of the joint. In between these bands will be polycarbonate. The goniometer will be in the middle of this polycarbonate and will press against the joint. The feedback module will be placed inside an elastic band and can be attached to any part of the body. Both modules will be worn by the user above or under clothing and will have to communicate with the user's smartphone, which will run Android OS version 4.3 or later in the first implementation and iOS in future implementations. Neither module will be more than 2m separated from the smartphone. There will be two modes of feedback during training sessions (from high to low implementation priority):

1. Feedback after/during an exercise through a smartphone.

2. Direct feedback during the exercise by means of a measurement module, feedback module and an algorithm.

Furthermore there will be another mode of feedback after training session via a web application.

2.2.2. Design specifications

To fulfil the clients desires, a list of requirements has been made which the client agreed on. The list of specifications that was agreed upon has been divided under several subsections that are clarified below.

Accuracy and reliability

- Measurement frequency of 100 Hz.
- Angle measurement with a resolution $\leq 0.1^\circ$.
- Measured angle may deviate from the real angle by $\pm 10\%$ of the real angle.

Magnetic decoder One of the following magnetic encoder has to be used: AMS5600 or AMS5601.

IMU An IMU with at least the same capabilities of the IMU used in the iPhone 4S. However an iPhone 4S uses a separate accelerometer (LIS331DLH) and gyroscope (L3G4200D). The specifications of both the accelerometer and the gyroscope are found below:

Accelerometer

- I2C/SPI digital output interface
- 16 bit data output (3-axis) at rates variable from 0.5 Hz to 1 kHz
- Dynamic $\pm 2g/\pm 4g/\pm 8g$ scales
- Independent programmable interrupt generator, build-in sleep to wake-up function

Gyroscope

- I2C/SPI digital output interface
- 3-Axis angular rate sensor
- 16 bit data output at four different output rates (100/200/400/800 Hz)
- Three selectable scales: 250/500/2000 degrees/sec
- Embedded power-down and sleep mode

The IMU that is used in the goniometer must be able to detect a peak and generate an interrupt. This would require immediate processing. The gained IMU data should be saved and should be able to be retrieved after training sessions.

Interface The goniometer, feedback module and the smartphone together form the total interface. The goniometer and feedback module should have some way to be turned on/off and a way to connect to the smartphone via Bluetooth Low Energy (BLE), for instance a button. Table 2.1 gives an overview of the different kinds of indications and the different input/outputs needed. (X) means optional.

	Smartphone	GonioTrainer
On/off indication	(X)	X
Measuring indication	(X)	X
Low battery	X	X
Start/stop measuring	X	
Adjust feedback settings	X	
Update algorithm/firmware	X	(X)
Charging indication		X

Table 2.1: Whether the indicator should be on the smartphone or GonioTrainer for different modes.

Communication

- Wireless connection between Smartphone and goniometer and between smartphone and feedback module.
- Haptic feedback should be given, with the use of a vibration motor, within a time period of 50ms after detection that feedback should be given (for example placement of skate).
- Multiple GonioTrainers may not interfere with each other.
- Preference lies with the nRF51822 SoC of Nordic Semiconductors for the sensor and feedback module.
- All modules, including smartphone, will have a maximum distance of 2m between them when in use.

Feedback module

- Intensity of feedback should be adjustable (length and amplitude of vibration).
- Vibration duration adjustable from 0.2ms to 0.4ms and amplitude should be no less than 5g.
- Feedback mode which allows for quick successive pulses.
- Burst duration of 65 ms and inter burst duration of 35 ms.
- Use of PicoVibe 9mm or Precision Haptic 8mm.
- The motor will vibrate a maximum of 900 times during a 1.5 hour training.

Costs and ease of development

- Finals costs per product below 100 Euros, where electronics may not exceed 60,-. First batch of 10 below 2500 Euros, and 100 below 10.000 Euros.
- Use of open source technology.
- Use of as much proven solutions and technology.
- One development environment.
- Different suppliers to reduce dependency.

Battery

- Enough capacity for 3 hours running time.
- Battery and charging circuit should comply with safety standards described in IEEE 1725.

Size, weight and housing

- Goniometer: size: $10 \times 35(\pm 5) \times 60(\pm 5)$ mm, and overall maximum volume of 21000 mm^3 . Weight: $\leq 67\text{g}$.
- Feedback module: size: $10 \times 17.5(\pm 5) \times 30(\pm 5)$ mm, and an overall maximum volume of 5250 mm^3 . Weight: $\leq 33\text{g}$.
- The goniometer and feedback module should be water resistant, which means at least IP67.
- Due to being water resistant, the goniometer and feedback module may each have a maximum of 1 physical port.

Environment of use

- The temperature range in which the GonioTrainer will be used is -10°C to $+40^\circ\text{C}$.
- The GonioTrainer will be used in damp, sweaty and/or wet environments.
- The GonioTrainer may be subject to mechanical abuse due to e.g. falling athletes.

Other

- Life span of the GonioTrainer minimal 3 years.
- Software should be up-datable through smartphone.
- Enough onboard memory for 3 hours of data logging.

2.3. The Task/Objective

The system will be designed and implemented by a BAP-group of six students, which is divided into three subgroups and each will be assigned a part of the system to design. The tasks have been divided in the following manner:

- Group 1, which consists of the authors of this thesis, will be in charge of the power supply, which entails making sure that all components are supplied with sufficient power at the right voltage and giving information about the battery's status. Furthermore they will design the feedbackmodule, but excluding the communication link and peak detection algorithm.
- Group 2 will implement the communication link between the modules and the smartphone via Bluetooth Low Energy.
- Group 3 will be in charge of reading and logging the sensor values, implementation of a peak detection algorithm and a controller.

Some aspects of the system, such as the connection architecture for direct feedback, has been discussed and chosen as a team at the start of this project and thus these design considerations will also be included in this thesis.

3

System Concept

3.1. System Architecture

In this section the options for the system architecture will be discussed to give an idea of what subsystems, and thus also which components, are needed.

3.1.1. Connection Architecture

Currently smartphones are a very widespread device. Smartphones are a bulk of information and processing power, conveniently put together in a small device. Therefore the client would like the GonioTrainer to work in conjunction with a smartphone. This leaves a couple of design choices on how to implement the direct feedback algorithm. In the following options, raw data is defined as data output of the IMU and the angle sensor.

1. The smartphone receives all raw data (except for feedback moment detection) from the goniometer and decides upon feedback or not. It sends the outcome of this decision to the goniometer. The goniometer determines the moment of feedback (e.g. when the user puts his/her foot down). The goniometer sends a signal to the feedback module to drive the vibration motor.
This architecture has the advantage that the smartphone only has one connection and the most of the processing will happen on the smartphone, lowering the need of processor power of the processor on the goniometer (and thus also the price). The disadvantages are that the goniometer should have two connections and direct feedback can not be achieved without using the smartphone during the physical activity.
2. The smartphone receives all raw data (except for feedback moment detection) from the goniometer and decides upon feedback or not. It sends the value of this decision to the feedback module. The goniometer still determines the moment of feedback and sends it to the feedback module. This means the feedback module now too will have to make a decision, because it should only vibrate when both incoming signals are true.
This architecture has the advantage that most of the processing happens on the smartphone and the latency between the detection of the feedback moment and driving the motor is shorter compared to when the smartphone has to send information to the goniometer first. The disadvantage is that there are more communication lines compared to the other architectures; the smartphone, goniometer and feedback module each has to maintain two connections in this triangle architecture. Furthermore direct feedback can not be achieved without a smartphone.
3. The smartphone receives all raw data (except for feedback moment detection) and decides upon feedback or not. It also receives the moment of feedback from the goniometer. The smartphone then sends a signal to the feedback module to drive the vibration motor.
This architecture has the advantage that only the smartphone, which probably has a high processing power, must maintain two connections. This architecture has the disadvantage that after the detection of the feedback moment, the signal to give feedback must first go to the smartphone and then to the feedback module, thus increasing the latency compared to when the signal goes directly from the goniometer to the feedback module.

4. The goniometer determines both the moment of feedback and feedback itself. It also sends a signal to the feedbackmodule to drive the vibration motor.

This architecture has the advantage that no smartphone is needed for direct feedback, there is only one connection line and probably has a latency compared to option 2. The main disadvantage is that the processor power on the goniometer should be higher compared to the other architectures and with a smartphone's processing power there are more future possibilities for more complex feedback algorithms.

These options all have their advantages and disadvantages. Implementing the feedback algorithm on the smartphone facilitates updating the algorithm since there are less restrictions due to a better processor. Furthermore updating the algorithm on a smartphone is more user friendly than updating the algorithm on a chip. The client has a preference for option 3 since this is a more simple product. A look will be taken at the BLE throughput to see if the 50ms time interval between feedback moment detection and motor driving can be achieved.

Bluetooth Low Energy can achieve it's low power consumption by going into a low power idle state between data exchanges. These data exchanges can not perform continuously, but have an interval (called the connection interval) between them which can be set from 7,5ms to 4s. Per connection interval, the nRF51822 can transmit a maximum of up to 6 data packets and each has a maximum of 20 bytes of user data [1]. Assuming that the data to be transmitted can fit in these 120 bytes and the lowest connection interval is chosen, the latency due to BLE from goniometer to smartphone to feedbackmodule will be 15ms. This leaves us 35ms for latencies in the circuits. Additional information about implementing BLE in Android and iOS has been sought. This project implements the system for Android, but the client has stated that he would like to eventually be able to bring the product to iOS. The minimum connection interval for iOS is 20ms, or 11.25ms if BLE HID is one of the connected services [2]. For Android 7,5ms can be achieved, but due to host limitations both Android and iOS will usually have a maximum of 4 packets per connection interval [3]. In conclusion, it will be assumed that the time window of 50ms can be achieved with architecture option (3) when using Android, but it is unsure for iOS.

3.1.2. Power management

There will be two modules that will need their own power supply. The power supply will need to consist of the following:

1. Battery to supply energy.
2. A charger if rechargeable batteries are chosen (The client has not specified that the battery must be rechargeable).
3. DC-DC converter if the battery voltage range is out of the supply voltage range for one of the components.
4. Battery gauge to monitor the battery's status.
5. Protection circuit to protect the battery from over discharge and short circuits.

A draft of the block diagram of the system can be seen in Fig. 3.1.

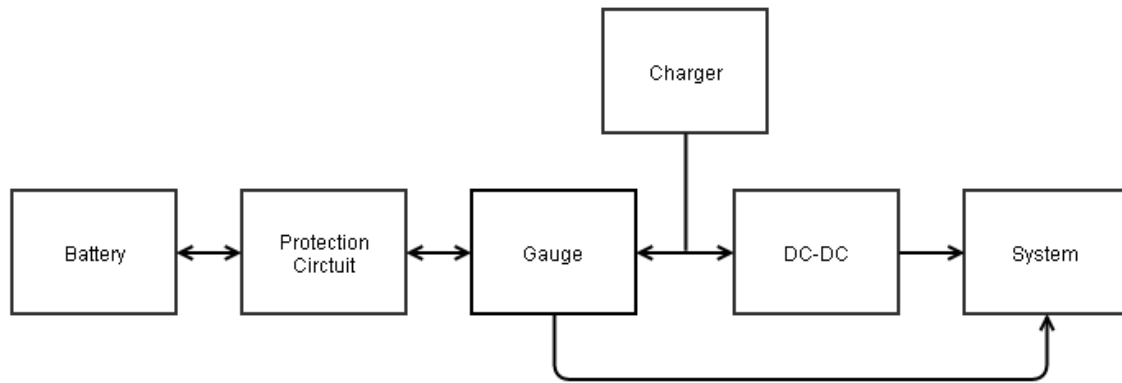


Figure 3.1: Block diagram of the power supply system. Arrows indicate power/information direction

3.1.3. Sensors

In order to measure the joint angle of the joint where the goniometer is attached to, some type of sensor must be chosen. The client has run a trial test using the goniometer, in which they used a magnetic encoder, namely the AS5600 from AMS. They have given their preference for either the same sensor or another, quite similar one, the AS5601. The group responsible for the sensor has chosen the AS5601. Of interest is the required supply voltage and the required current. Both can be found in the datasheet and have a value of 3.0 - 3.6 V and 6.5 mA (max) respectively.[4]

The client has requested that feedback be given at most 50 ms after an ice skater places his/her skate. From their trial runs they have concluded that this would be too complex to determine from the knee angle alone. Therefore they have requested an inertia measurement unit (IMU) to be added as well. In the same trial run they had used the iPhone 4S. In section 2.2.2 the requirements for this IMU have been defined, by combining an accelerometer and a gyroscope. Keeping these in mind, the same group has decided upon the MPU6050 from InvenSense. Once again, the supply voltage and current are 2.375 - 3.46 V and 3.9 mA respectively [5].

3.1.4. Prototyping

In order to have either the goniometer or the feedback module perform an action, a microprocessor is required. The client has given their preference to the ISP130301 from Insight SiP. This is a System on a Chip (SoC). This SoC has a required supply voltage of 2.1 - 3.6 V. Because the ISP130301 is a SoC there are several modules which each requires a certain amount of current. All these modules are assumed to work on a stabilized 3.3V.

Device interface or peripheral	Description	Nominal current [mA]	3-hour Consumption [mWh]
16 MHz crystal oscillator	Run current	0.470	4.65
	Startup current	1.1	10.89
32 MHz crystal oscillator	Run current	0.500	4.95
	Startup current	1.1	10.89
16 MHz RC oscillator	Run current	0.750	7.43
CPU	Executing code from flash memory	4.1	40.59
	Executing code from RAM	2.4	23.76
	CPU startup current	0.600	5.94
Radio transceiver	TX only run current at $P_{out} = +4$ dBm	16	158.4
	TX only run current at $P_{out} = +0$ dBm	10.5	103.95
	TX startup current	7	69.3
	RX only current at 2 Mbps	13.4	132.66
	RX startup current	8.7	86.13

Table 3.1: Power consumption ISP130301 [6]

Not all of these modules will be used in conjunction and will thus not contribute during the regular running period. Moreover the startup currents take place in a matter of milliseconds. When comparing this to a 3 hour running period, it is safe to say that these are negligible. Therefore the total 3-hour consumption of the modules combined sums to: $4.65 + 4.95 + 7.43 + 40.59 + 23.76 + 158.4 = 239.78 mWh$.

3.2. Power Supply

There are two separate modules in the GonioTrainer, so each one will need their own power supply. But since the product may be used in mechanically abusive environments (an ice skater can fall at high speeds), special attention needs to be given to the safety of the batteries when mechanically abused. Furthermore the battery should be lightweight and small enough to fit in the specified dimensions. The following steps will be made in this design choice:

1. Approximation of the power consumption by each module.
2. Review of different available batteries. Take energy densities, specific energy and safety into account.
3. Contact client if there are specifications that can not be met and propose alternatives.
4. Choose battery.
5. Choose charging method and circuit design, if applicable.

3.2.1. Power consumption

Components goniometer	Supply voltage range [V]	Components feedback module	Supply voltage range [V]
ISP	2.1 - 3.6	ISP	2.1 - 3.6
IMU	2.38 - 3.46	Motor driver	2-5.2
Angle sensor	3.0 - 3.6	9 mm motor	0.3-3.6
Memory	2.7 - 3.6	8 mm motor	0.8-5.4

Table 3.2: Supply voltage ranges of the components

To preserve space and power, one would like to have as less voltage converters as possible, since these are not 100% efficient. So an operating voltage has to be defined for all or most components of a module. In table 3.2 the operating voltage range of the components, derived from the corresponding data sheets, can be observed. The lowest minimal and maximum supply voltage that does not fall out of the ranges of all components sets the range in which the supply voltage can be set. For the goniometer, this range is 3.0-3.46 V. To lower the stability requirement of the supply voltage, the operating voltage will be chosen with some margin between the maximum and minimum of the range. For the goniometer this is chosen to be 3.3 V, because this is a common level that is used and thus many fixed DC-DC converters are available for this. Due to the ease of using the same DC-DC converter and because it is possible, this same operating voltage level will be used for the feedback module.

Components goniometer	Nominal current [mA]	Nominal voltage [V]	3-hour Consumption [mWh]
ISP	24.22	3.3	239.78
IMU	3.9	3.3	38.61
Angle sensor	6.5	3.3	64.35
Memory	30	3.3	297
	64.62		639.74 Total

Table 3.3: Power consumption goniometer

The specifications state that the product should be able to operate 3 hours without recharging. However either vibration motor requires a startup current which is significantly higher than the nominal rated current. A typical step response for the Precision Haptic 8mm can be seen in Fig. 3.2.

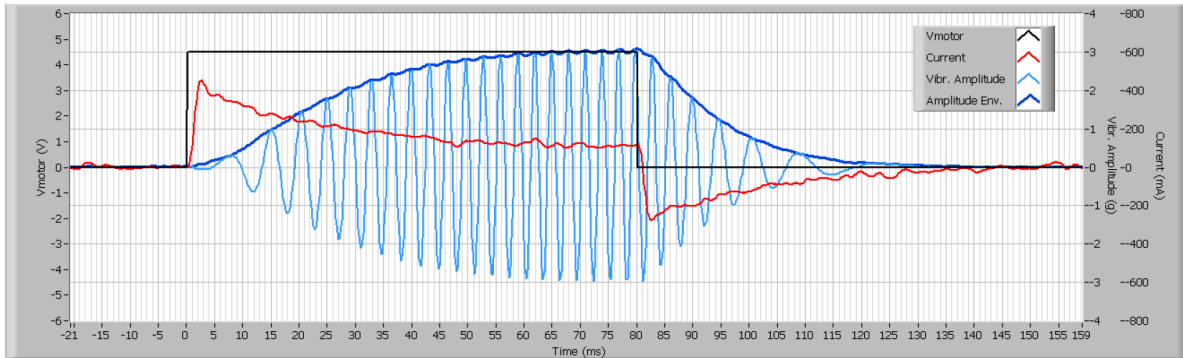


Figure 3.2: Typical step response for a DC vibration motor from Precision Microdrives (Picture from Precision Microdrives)[7]

What should be taken from Fig. 3.2, is the fact that the peak current (the red line) is at its nominal rated current after $\sim 50ms$. With this given, the 3 hour consumption in mWh can be calculated. The area underneath the red line times the rated voltage equals the power consumed in joule for however many seconds was taken. The length of vibration was agreed with the client to be $0.2 - 0.4s$. The maximum number of times feedback should be given was also agreed upon, namely 900 in an hour and a half. In the worst case scenario the motor has to vibrate continuously during $0.4s$. This amounts to:

$$\text{area under red line} \times V_{rated} \times 1800 = 0.065 \times 4.5 \times 1800 = 523.46J = 145.41mWh \quad (3.1)$$

From here on the mode in which the motor will vibrate continuously will be referred to as constant mode. The motor should be able to vibrate in the following way when pulsing: pulse width of $65ms$ and inter pulse width of $35ms$. All in the same time span of the same $0.2 - 0.4s$. This gives for the consumed power once again the area under the red line in $65ms$ times the rated voltage for the power consumed in $65ms$ in joule. This needs to be multiplied by four, for the total power consumed in $0.4s$. For the 3 hour duration we multiply this by 1800 to find the total power consumed in 3 hours using pulse mode:

$$\text{area under red line} \times V_{rated} \times 4 \times 1800 = 0.01605 \times 4.5 \times 4 \times 1800 = 520.02J = 144.45mWh \quad (3.2)$$

These calculations are the same for the Precision Haptic 9mm. However this motor does not have a typical step response graph like the 8mm does. Therefore it is assumed that the characteristics are the same, but for instance the peak current, rated voltage, etc., are adjusted to the specified peak current. This yields the following results for the 9mm motor in constant mode:

$$\text{area under red line} \times V_{rated} \times 1800 = 0.05 \times 3 \times 1800 = 270J = 75mWh \quad (3.3)$$

And for pulse mode:

$$\text{area under red line} \times V_{rated} \times 4 \times 1800 = 0.0165 \times 3 \times 4 \times 1800 = 356.4J = 99mWh \quad (3.4)$$

Components feedback module	Nominal current [mA]	Nominal voltage [V]	3-hour Consumption [mWh]
ISP	24.22	3.3	239.78
9mm motor nominal	100	3	99
8mm motor nominal	145	3.3	145.41
	124.22		338.78
	169.22		385.19
			Total_{9mm}
			Total_{8mm}

Table 3.4: Power consumption feedback module

In table 3.3 and table 3.4 the power consumed in 3 hours by each component of the goniometer and feedbackmodule, respectively, can be observed. Since all the components will be connected in parallel, the total current, which needs to be supplied by the power supply, is the sum of all these currents, according to Kirchhoff's current law.

3.2.2. Review batteries

A choice has to be made between primary and secondary batteries. Primary batteries are not capable of being easily or effectively recharged electrically and, hence, are discharged once and discarded. Secondary batteries can be recharged electrically, after discharge, to their original condition by passing current through them in the opposite direction to that of the discharge current. An overview of batteries made from different compounds can be found in Fig. 3.3 and 3.4, along with the energy densities and specific energy.

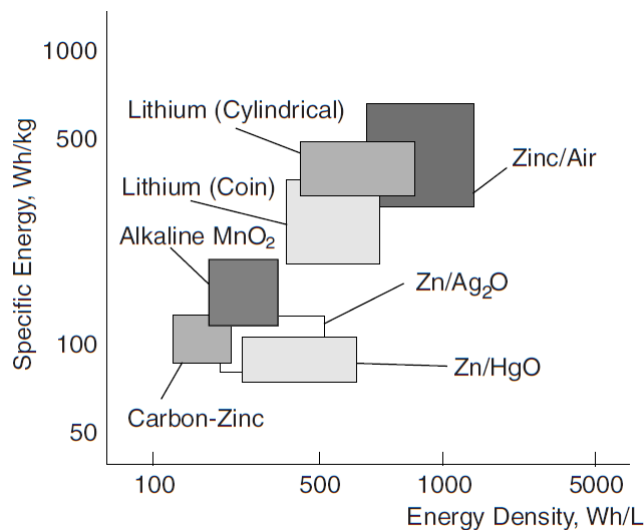


Figure 3.3: Energy densities of primary batteries [8].

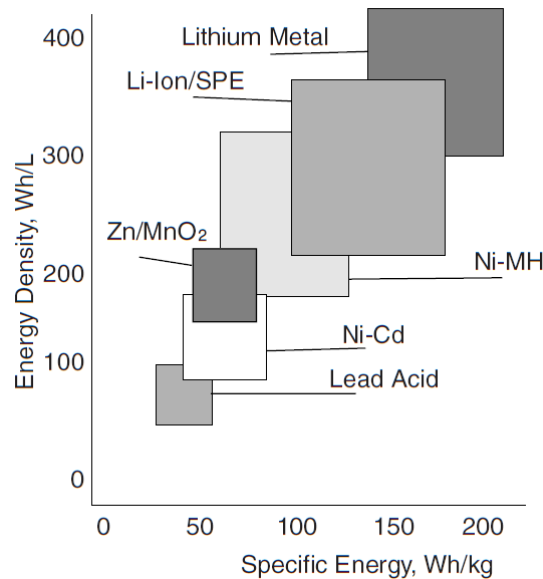


Figure 3.4: Energy densities of secondary batteries [8].

Ideally, you want to be as high as possible on the 45 degree curve to get both a small and and lightweight battery with the most energy. The general advantages of primary batteries are good shelf life, high energy density at low to moderate discharge rates, little, if any, maintenance, and ease of use. The vast majority of primary batteries are the familiar single cell cylindrical and flat button batteries or multicell batteries using these component cells. Secondary batteries are characterized (in addition to their ability to be recharged) by high power density, high discharge rate, flat discharge curves, and good low-temperature performance. Their energy densities are generally lower than those of primary batteries and their charge retention is also poorer than that of most primary batteries [8].

Batteries come in all kinds of forms and shapes for non cosmetic reasons. The shape of a battery has a lot to do with ease of production, safety measures and the capable amount of energy stored.

3.2.3. Cylindrical cell

As of yet these kind of batteries are still the most used, because they are manufactured easily and are mechanically stable. Most lithium and nickel based cylindrical cells come with some safety measures. They usually have a positive thermal coefficient (PTC) switch, which will become highly resistive when exposed to high currents, acting as an overload protection. When the current drops, the PTC will cool down and become conductive again. Cylindrical cells usually also have a pressure relief system, which consists of a membrane seal which will break under high pressure. A downside is that these cells cannot be stacked neatly and will leave some room unused due to the shape [9].

3.2.4. Button cell

Generally button cells, also known as coin cell, are very small and inexpensive to build. They have no safety measures however and can swell when charged too quickly. Moreover they can usually only be charged at an 10 to 16 hour rate. Should they have to provide more than 30 mA for short periods of time, the capacity will reduce significantly. Most button cells are not rechargeable and have no safety vent [9].

3.2.5. Prismatic cell

These cells make good use of their space by using a layered approach. Prismatic cells will need some form of housing, as they are less mechanically stable than the cylindrical cell. They may swell a little due to gas buildup[9].

3.2.6. Pouch cell

In this kind of battery conductive foil-tabs are welded together to the electrodes and are fully sealed on their way to the outside of the battery. Pouch cells make the most efficient use of space, a 90-95% packaging efficiency, the highest among battery packs. The same as prismatic cells, these lack mechanical stability, thus they will need some support. They may very well swell some as well, 8-10% swelling over 500 cycles is normal.

Both the prismatic and the pouch cell could one day surpass cylindrical cells in the energy holding department, but due to the technology not being mature yet, this is not true as of yet [9].

3.2.7. Conclusion

As can be seen from Table 3.3 and 3.4 batteries with at least 640 mWh and 340 or 390 mWh will be needed for the goniometer and the feedback module respectively. Since cylindrical cells are usually no smaller than 15mm in diameter, a prismatic cell or pouch cell is the only viable option left in order to meet the product size demand.

3.3. Battery Protection

The battery will need two kinds of protection, one from physical abuse and protection against over-(dis)charging and currents too large for the battery to handle. The latter is battery specific and can be found in the corresponding datasheet. However, each battery chemistry has their own maximum (dis)charge voltage. With regards to physical abuse, an, e.g., ice skater may very well not make the turn and slip. Should the skater fall on the GonioTrainer, it is preferable for the battery to not explode or overheat. Unfortunately, the high density, small secondary batteries are also the unsafest because they usually lack safety measures in order to make the most efficient use of available space. After having discussed this with the client, they have agreed to use a high density relatively unsafe battery and that they will have to design a casing strong enough to withstand some physical abuse. Moreover, when looking at other devices that require power supply in the form of a battery and need to be able to withstand physical abuse, the GoPro comes to mind. The GoPro is a camera used in conditions a regular camera would fail, think skiing, mountain biking, surfing, swimming, skydiving, etc. Not only is it water resistant, it is also fairly resistant to physical abuse. The interesting part is that the official GoPro battery is a LiPo battery, just firmly encased. The wrapped in battery however, is only shielded by the GoPro itself by a thin plastic cover.

3.4. Battery Charging

Lithium Ion batteries have an anode that consists of the lithium metal. Lithium ions move from the anode to the cathode, hence the name Lithium Ion (Li-Ion or Li+). Li-Ion Polymer (LiPo) batteries come in the pouch format. However LiPo can be confusing. When the LiPo battery was a new phenomenon, the polymer indicated the polymer electrolyte instead of the liquid electrolyte. This resulted in a "plastic" cell. Later manufacturers began calling the Li-Ion in the pouch format LiPo, which is the most common form nowadays. It indicates the polymer casing, rather than the polymer electrolyte [10]. This kind of chemistry requires a special kind of charging the cell, because when overcharged too many lithium ions are removed from the cobalt-oxide lattice that it disintegrates. If this happens there is change that small amounts of lithium metal form which can make the battery unstable and therefore dangerous.

On the other side of the spectrum there is the overdischarged state. Should the cell fall below its rated maximum discharge voltage results in progressive breakdown of the electrode materials. The anode copper current collector will be dissolved in the electrolyte. This will increase the self discharge of the cell. Whenever the cell's voltage will be raised above the maximum discharge voltage, the copper ions, which have been dispersed throughout the entire electrolyte, will be precipitated as metallic copper. This could cause a short circuit between the electrodes[11]. Should the cell be recharged, a lot of capacity will be lost. Motorola Mobile Devices has done research on this subject. Cells were overdischarged and kept at 2.0, 1.5, 1.0, 0.5 or 0.0V for 72 hours and then cycled five times, which means discharging to 3.0V at 0.4A and subsequently charged to 4.2V at 0.8A. This was repeated five times. Cells overdischarged between 2.0 and 0.5V lost a permanent 2-16% of their total capacity. Said cells lost an additional 8-26% after they'd been cycled a 100 times between 4.2 and 3.0V at 0.8A.[12]

Even though less dangerous, not fully charging the cell by as much as 1.2% of its optimum full charge voltage lowers the capacity by 9%. Therefore to get the most out of a cell, recharging it to its optimum full

charge voltage is desired. In order to do so a certain charging method called constant current/constant voltage (CC/CV) was developed. This means to apply a constant current with varying voltage and end the charge cycle with a constant voltage and a diminishing current.

This sequence starts with checking whether the cell hasn't been deeply discharged, which means a voltage $< 3V$. Should this for some reason be the case, a small current will be applied, around 10% of the full charge current, to make sure the cell will not overheat. When the cell is finally ready to accept the full charge current, the CC mode is entered, which means charging at 1C. C stands for capacity, so a 2Ah cell will have a 1C current of 2A. This is continued until the cell has reached 4.1V. Charging at 1C will take about one hour, but will not leave the cell fully charged. Charging at less than 0.18C is optimal, but will take slightly longer than 5 hours to fully charge.

When 4.1V has been reached, the constant voltage mode is entered to avoid the risk of overcharging. During this mode the current will drop to 1C. This is when charging is done. Should the charger remain connected a periodic charge is applied to counteract the battery self discharge[13]. This entire sequence can be seen in Fig. 3.5.

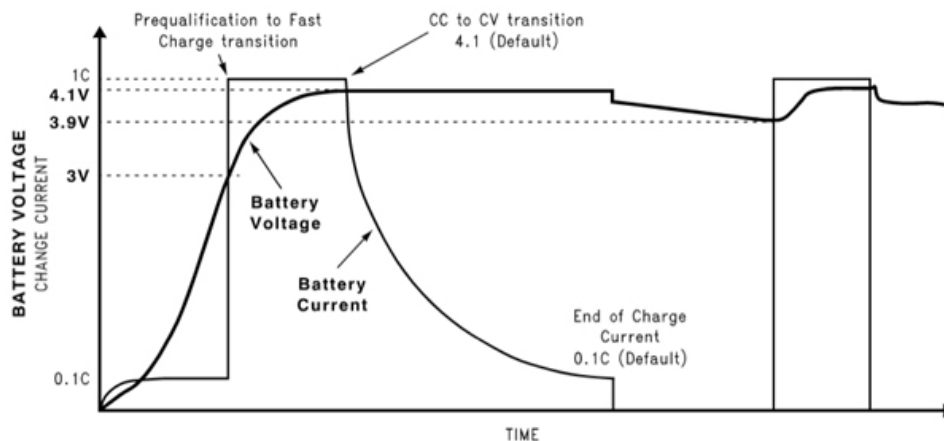


Figure 3.5: Li-Ion charging profile. Starting from a deeply discharged state, a small current is applied, then constant current mode is entered. At 4.1V constant voltage mode is entered. Afterwards a periodic charge is applied to counteract cell self discharge. (Picture from National Semiconductor)

There are three methods that can be used to charge a Lithium-Ion battery, namely linear-, switch- and pulse-mode, each with its own advantages and disadvantages. The major differences between these modes are the size and cost vs. performance trade off. Moreover linear chargers are usually preferred when dealing with low charging currents and single cell batteries[14].

3.4.1. Linear chargers

A simple way to charge a battery is by using a linear charger. This kind of charger requires little size and complexity. It uses a pass transistor operating in its linear region to drop the voltage down to the battery level. Just a couple of external components are needed: an in-, and output bypass capacitor, resistors for setting voltage and current limits and sometimes another pass transistor.

This of course sounds well enough, however, linear chargers have a high power dissipation. As mentioned, the charger uses a pass transistor to simply drop the voltage down to the required battery voltage. The power dissipated is the charger voltage (5V from USB) minus the battery voltage (2.75 – 4.2V) times the charger current. When dealing with LiPo batteries charging at high currents ($\sim 1A$) this could mean a potential power dissipation of roughly 3W[15].

3.4.2. Switching chargers

Where linear chargers have more power dissipation, switching chargers have consistently low power dissipation over a wide range of input and battery voltage. Another advantage switching chargers have, is that they allow the use of a smaller and cheaper AC wall adapter than a pulse charger, because they perform well over their wide input voltage range.

However, this kind of charger has its downsides: its size is remarkably larger than the linear and pulse mode chargers plus its complexity is higher. Because it's more complex, it requires more space for it

external switches and filters. Additionally, as the name would suggest, the switching action generates electromagnetic interference and electrical noise. This switching is done at a fixed frequency and so this generated noise could be easily filtered, but this will require even more external components[15].

3.4.3. Pulse chargers

The last type of chargers have advantages of both the other chargers. It's efficient like the switch mode charger and small like a linear charger, because it does not require an output LC filter. When the battery being charged by a pulse charger is low, the pass transistor will conduct which will supply the source current directly into the battery. When the regulation voltage is reached, the input current is pulsed to achieve the desired charging current. When this portion of the charge cycle is reached, the pass transistor is not in its linear region, unlike the linear charger, thus the dissipated power will be lower. But once again, there is a downside. The input voltage source needs its own current limiter, as this charger will not take care of that. This current needs to be precisely defined.[15].

3.4.4. USB compatibility

Nearly every modern device has a USB input. Not only can USB transfer data, it can also be used to power/charge your device. USB 2.0 can supply $5V \pm 0.25V$ and a maximum current of 2A. As was just explained a LiPo battery will need a voltage as high as 4.2V. USB2.0 has 4 pins, two for power supply (named V_{BUS} and GND) and two for data transfer (named D- and D+). However the data pins can be left unconnected if no data transfer is needed[16].

3.4.5. Power path management

Say the user would want to use the device whilst it is being charged, but the battery is all out of charge. Should the load require more power than the charger is supplying, the device would not turn on nor be charged. Another issue would be for the battery to have almost completed charging, but an LED for instance would keep drawing power from the battery. This would essentially mean the battery would never be fully charged. It would thus be ideal if the power supply feeding the battery charger, could also power the device so that the device would not need the battery's charge while it is being charged.

3.5. Low Battery Indication

The client has requested some visual indication of a low charge battery. Since it is nothing more than an indication of a low charge battery, the voltage profile of a LiPo battery could be used as an indicator for the amount of charge left.

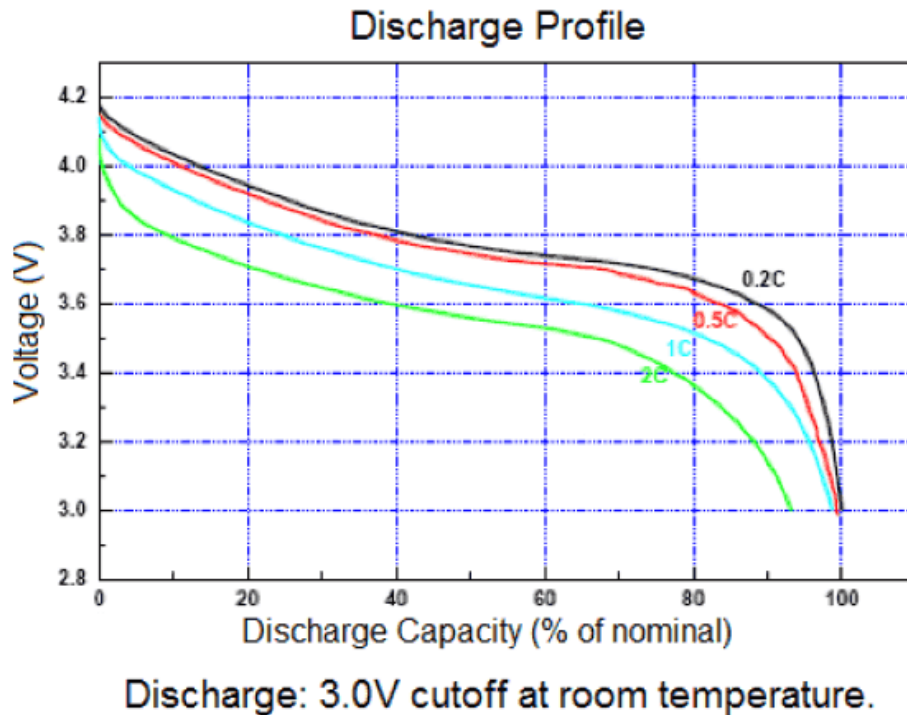


Figure 3.6: A typical voltage profile for a LiPo battery at room temperature, drained at various discharge rates. (Picture from Adafruit)

However this is highly dependent on battery manufacturer, temperature, etc., and would thus only be a very rough indication. Another problem with this approach would be that when a discharge current is applied, the voltage will drop. This can be seen in Fig. 3.6. Moreover, the voltage has a long plateau, from which it will be very hard to estimate the State of Charge (SOC). For accurate readings, the battery would have had to rest for four hours. Then how can we measure the SOC of a battery? A battery is usually thought of as some sort of fuel tank, which isn't wrong in its entirety, it's just that there are a lot more factors to a battery than to a simple fuel tank. To estimate the SOC of a regular fuel tank, a fuel gauge measures the in and out going liquid from a tank of known size. However, for a battery, the size of the "tank", if you will, will shrink a small percentage of its maximum size after each charge cycle. A fuel gauge can give more precise information about the battery; it measures current, voltage, temperature and absolute and relative capacity using a specifically designed method. Multiple battery fuel gauge manufacturers have designed their own method of calculating the SOC [17].

3.5.1. Coulomb counter

The classic SOC determination method uses coulomb counting. This method connects a sense resistor in the charge and discharge path of the battery. An ADC measures the voltage across this resistor and then passes the current value to a counter. A real time counter (RTC) is used to calculate the integral of the current for the value in coulomb. A coulomb counter alone can provide information about the remaining capacity, full charge capacity and remaining time till empty or full. A coulomb counter isn't perfect however, because it will accumulate the offset error in the current sense and the ADC measurement. Although small, over time it will increase. In order to prevent this, three flags are made: End of Charge (EOC), End of Discharge (EOD) and relax. When a battery is fully charged, the EOC flag will be set and thus the SOC should be 100%. Similarly, when a battery is fully drained under discharge, the EOD flag will be set and thus the SOC should be 0%. Relax is when the battery is not being charged or discharged.

Another factor to take into account is the batteries real full charge capacity (FCC) and the error thereof. The FCC is highly dependent on ageing, temperature, load, etc. It is essential to either recalibrate the battery every 3 months, or to include some parameters into calculations to compensate for this factor [18].

3.5.2. Dynamic voltage-based fuel gauge

The company RICHTEK has developed another method of calculating only the SOC using the battery voltage only. This works for Li-Ion batteries only. The way this method works is it estimates the increasing or decreasing SOC using an iterative model, according to the difference between the battery voltage and the open circuit voltage (OCV). Compared to the coulomb counter method, the voltage based fuel gauge cannot have an error due to current sense error or battery self discharge. This method can improve its SOC estimation by a learning cycle which consists of fully charging to fully discharging the battery. The method has a maximum error of about 3% [18].

3.5.3. ModelGauge m3

The company Maxim Integrated Products also developed their own kind of battery fuel gauge method. It combines a coulomb counter with a voltage fuel gauge (VFG). The VFG estimates the OCV and simulates the internal dynamics of a Li-Ion battery to determine the SOC. This way the SOC estimation does not accumulate offset error over time. Moreover, it weighs the result from both the VFG and the coulomb counter to determine the battery state. This information is then used by the ModelGauge m3 algorithm to determine the remaining capacity, taking temperature, current, age and application parameters into account. Over time, the change in capacity is monitored and the VFG will adapt to this change [19].

3.6. DC-DC Converter

To convert the varying voltage of the battery to a constant level suitable for the used component, a voltage regulator should be chosen. Since the voltage of a Li-ion battery can go from 4.2V to 2.7V and the desired level will be 3.3V, the regulator must be able to drop as well boost the input voltage if the battery should be used below the output voltage level.

3.6.1. Linear regulator

A linear regulator can be thought of as a resistor voltage divider, but with a regulated variable resistance. This variable resistance is created by operating a bipolar or field effect power transistor in its linear mode, thus the transistor acts like a resistor [20].

The advantages of a linear regulator is that they are very simple to use and need few external components to work properly (e.g. the LT1083 that was developed twenty years ago: it only needs an in- and output capacitor and two feedback resistors to regulate the output voltage). Furthermore they are relatively cheap and can be more efficient than switching regulators when the output voltage is close to the input voltage.

A major drawback of these type of regulators is the power dissipation in the series transistor operating in linear mode. Since the load current must pass through this resistor, the power dissipation [W] is equal to: $P_{Loss} = (V_{in} - V_o) * I_o$. Where $V_{in}[V]$ is the input voltage, $V_o[V]$ the output voltage and $I_o[A]$ the load current. An estimation of the efficiency is then:

$$\eta[\%] = \frac{P_{Output}}{P_{Output} + P_{Loss}} = \frac{V_o I_o}{V_o I_o + (V_{in} - V_o) I_o} = \frac{V_o}{V_{in}} \quad (3.5)$$

Where $P_{Output}[W]$ is the output power [20]. Furthermore linear regulators are only capable of dropping the voltage to a lower level, so boosting will not be possible with this type of regulator.

3.6.2. Switching regulator

Switching regulators can efficiently regulate the output voltage by operating a power transistor in conjunction with an inductor. The advantage of a switching regulator is that they are efficient (up to 96%) under many combinations of input voltages and load currents [21]. So they are efficient when the input and output voltage differ a lot in magnitude. There are different topologies for different uses.

1. The buck converter is used for stepping down the voltage.
2. The boost converter is used for stepping up the input voltage.
3. The buck-boost converter is used for stepping up as well as stepping down the voltage level.

The drawback of switching regulators is that they usually need more external components and thus consume more board area, are more expensive and generate more noise than linear regulators [21]. Furthermore they can produce RF noise at high switching frequencies.

3.6.3. Charge pump

Charge pumps perform the same functions as switching regulators, but instead of an inductor, capacitors are used to step up, step down or boost the input voltage. Charge pumps come in both regulated and unregulated form. For this application regulated charge pumps are suitable since the load and input voltage may vary and a constant output voltage is desired. Charge pumps have the advantage that they are cheaper and produce less noise than switching regulators. The disadvantage is that they have an upper output current limit of about 125mA. There are a few IC's that deliver output currents in several hundred mA, but it is not economical to build such pumps so inductor-based switching regulators are better suited [21]. Furthermore when looking at IC's it resulted that the efficiency of charge pumps vary greatly (30%) with the input supply voltage and the voltage of batteries, can vary greatly during a discharge cycle.

3.7. Motor Driving

For the feedback module a vibration motor has to be driven. In the specification a choice between two ERM (eccentric rotating mass) motors is given. An ERM is a DC motor with an asymmetric mass on the shaft. Due to the centripetal force of the mass being asymmetric, there is a netto force caused by the centrifugal force. This force results in vibration [22].

It should be possible to change the amplitude of the vibration and this can be achieved by increasing the power to the motor. To understand this we will take a look at the equivalent model of a DC motor, depicted in figure 3.7.

The winding inductance L is defined by the mechanical design of the armature. It tries to prevent the current reversal. The winding resistance is modelled as a series resistance R . The electromotive force (EMF) is the voltage that is set on the motor terminals when the shaft is rotating. The relationship between the EMF[V] and the shaft speed is defined as:

$$EMF = K_v \omega \quad (3.6)$$

Where $K_v[\text{rad/s/V}]$ is the motor velocity constant and $\omega[\text{rad/s}]$ the shaft rotational speed. Using Kirchhoff's voltage law and the above equation, a steady state relationship between motor speed and input voltage can be derived:

$$\omega = \frac{V_{in} - RI}{K_v} \quad (3.7)$$

Where $V_{in}[V]$ is the input voltage, $R[\Omega]$ is the winding resistance and $I[A]$ is the current through the loop defined by the torque, $T[Nm]$, and motor torque constant, $K_T[Nm/A]$, as: $I = \frac{T}{K_T}$. So as the voltage increases, the speed of the motor increases proportionally. When the speed increases, the magnitude of the centrifugal force will increase exponentially as the relationship between this force and the speed is:

$$F_{centrifugal} = mr\omega^2 \quad (3.8)$$

where $m[kg]$ is the mass and $r[m]$ is the perpendicular distance from the axis to the centre of mass. A look will be taken at the different ways to drive an ERM motor. Output signals from digital microprocessors' ports are not designed to provide enough current for vibration motors, so driver circuits are needed to drive these motors [23]. Note that the client has stated that a series of short vibrations is more desired than a continuous vibration during feedback.

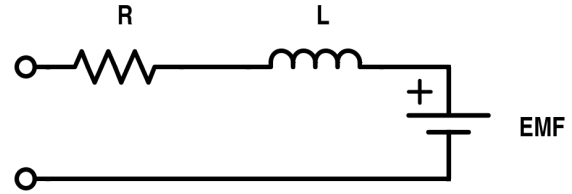


Figure 3.7: An equivalent circuit model for the DC motor

3.7.1. MOSFET with PWM

A PWM signal can be used to drive a MOSFET which in turn acts as a switch between a power supply, which can supply enough current, and the motor. By modulating the width of the PWM signal, the on-time of the switch can be varied and thus also the average voltage provided to the motor. An example of such a circuit is depicted in figure 3.8. The diode is used to eliminate flyback, which is the voltage spike that appears when the supply voltage is removed from the motor, which has an inductive element. The advantage of this approach is that it is relatively simple to implement and only needs a few components. The disadvantage is that active braking by reversing the voltage polarity requires feedback of the motor speed (to not reverse the motor) and thus more components and an increase in complexity. Active braking may be wanted if inactive braking takes longer than is desired.

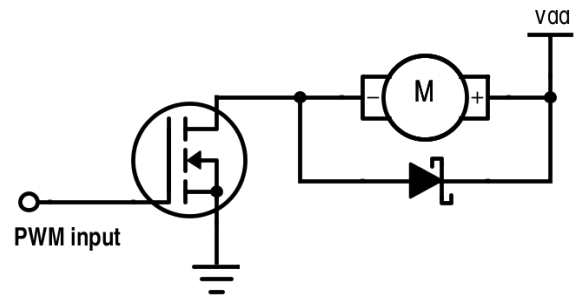
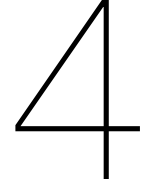


Figure 3.8: A driving circuit using a MOSFET

3.7.2. Driver IC

There are dedicated integrated circuits for variable driving of ERM motors. These IC solutions are usually more expensive than the solution described in section 3.7.1, but have their own regulation for braking. There are IC's that can take a PWM input to modulate the speed of the motor.



Implementation

In the previous chapter a block system for the GonioTrainer was drafted. In this chapter components will be searched and a complete power supply and feedback module will be implemented. Problems encountered during implementation and changes from the draft design will also be discussed.

4.1. nRF51822 Development Board

For prototyping with the nRF51822, the same development board used by the previous BAP group will be used [24]. This is the RedBearLab nRF51822 development board. The layout of this board can be observed in appendix A. The online mbed development environment was used along with the mbed libraries. Mbed is an online platform for prototyping with microcontrollers. The libraries are delivered "as is" and can be used for production at no cost[25].

4.2. Battery

As was said in section 3.2.7, the size and available capacity for batteries limits the choice to LiPo batteries. Taking a look at Tables 3.1, 3.3 and 3.4 will help make the correct decision for the battery. For the goniometer a battery of at least $639.74mWh$ is required. However batteries are usually measured by ampere-hours (Ah) instead of mWh, so when the nominal voltage of a LiPo battery equals $3.7V$, this amounts to $639.74/3.7 = 172.9mAh$. The feedback module requires, when used with the 8mm motor: $385.19/3.7 = 104.1mAh$ or when used with the 9mm motor: $338.78/3.7 = 91.6mAh$. These found capacities used in conjunction with the specifications from section 2.2.2, allows for specific battery selection.

A battery will lose some available capacity after each charge cycle. After 300 cycles only 80% of the rated capacity will be available. In three years time the goniometer and feedback module will be used for a total of 1.5 hours per training, 4 times a week, 52 weeks a year, 3 years long = 936 hours. The calculated capacities are for 3 hour usages. This means the total amount of times the goniometer or the feedback module needs to be recharged, when used at the nominal current that was calculated, will be $936/3 = 312$. This is more than the 300 cycles stated earlier, therefore a battery for the goniometer with at least $172.9 \times \frac{1}{0.8} = 216.13mAh$ will be needed. For the feedback with 8mm motor: $104.1 \times \frac{1}{0.8} = 130.1mAh$ and with 9mm motor: $91.6 \times \frac{1}{0.8} = 114.5mAh$. However, as can be read in section 4.5, the chosen buckboost will have an efficiency of 90%. Therefore these values need to be slightly higher, namely $240.14mAh$ for the goniometer and $144.56mAh$ and $127.22mAh$ for the 8mm and 9mm motor, respectively. These calculations were done assuming the entire capacity was drained in a 3 hour session.

For the goniometer a battery with at least $240.14mAh$ is required with a volume no larger than $10mm \times 2100mm^2$. By staying within the boundaries and being able to provide enough power for 3 hours of usage, the choice has fallen on the LP-402933-IS-3, with a typical capacity of $300mAh$ and volume of $3.8 \times 29 \times 34 mm$.

For the feedback module the choice has fallen upon the LP-402025-IS-3, with a typical capacity of $165mAh$ and size of $3.8 \times 20 \times 26 mm$, where the maximum volume is $10mm \times 525mm^2$ [26][27].

Both batteries fill almost the entire specified area. However, neither is even half of the thickness (10mm). It's assumed that the battery could be placed on top of the electronics and essentially leave the same area for the electronics. This assumption was made by looking at a different product, namely the ShotTracker. This device consists out of printed circuit board (PCB) and a battery on top of each other. With external casing, the total thickness is 6.6mm [28].

4.3. Battery Protection

As was read in the previous chapter, LiPo batteries will require over-(dis)charge protection. Luckily, most LiPo batteries have a protection circuit directly attached to the battery. As did the LP-402933-IS-3 and the LP-402025-1S-3.

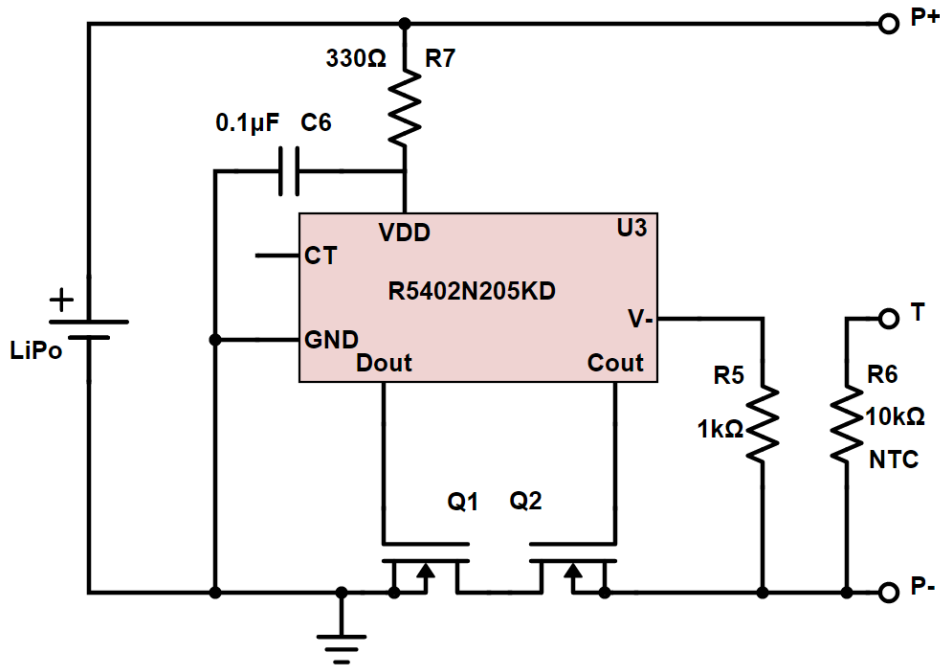


Figure 4.1: The protection circuit for the LP-443440-1S-3.

The IC in Fig. 4.1 is the Ricoh R5402N204KD. It works as follows: when over-charge voltage or over-charge current is detected, C_{OUT} switches to low, which is defined as the charger's negative pin level. It does so after a set delay. This will turn off the external N-channel MOSFET. C_{OUT} can be set to high again when a battery voltage lower than the over-charge voltage is detected, the charger is disconnected and a load is connected, in that order. This will turn the external MOSFET back on again. Something similar holds for D_{OUT} ; when over-discharge voltage or an over current is detected, D_{OUT} switches to low after a set delay. When this happens, a charger should be connected. When the battery supply voltage crosses the over-discharge threshold or when the battery voltage itself becomes greater or equal than the release voltage from over-discharge, the D_{OUT} pin becomes high again, allowing use of the battery once more.

The typical application can be seen in the schematic from Fig. 4.1. R7 and C6 are used to stabilise the supply voltage to the R5402. R7 and R5 work as a current limit when the cell is placed in the wrong direction or when excess charge voltage is applied. Finally R6 is an NTC which can be used to measure the temperature. This will not be used.

The values for the overcharge detection and release, and overdischarge detection and release, can be varied with the R5402N series by selecting a different part from this same series.

	R5402N204KD	R5402N205KD
Overcharge detection	4.2V	4.2V
Overcharge release	3.9V	3.9V
Output delay of overcharge	1.0s	1.0s
Overdischarge detection	2.5V	3.0V
Overdischarge release	3.0V	3.2V
Output delay of overdischarge	20ms	20ms

Table 4.1: Comparing the differences between the current battery protection IC and the preferred.

As can be seen from Table 4.1 both ICs are nearly the same, except for a small, yet important difference: the overdischarge detection. When a LiPo battery reaches a voltage of 2.5V nothing will happen just yet, but recharging it at this point may be dangerous. Therefore it is preferable for this not to happen. For this reason a slightly different part from the same series is chosen, namely the R5402N205KD. Both chosen batteries have a discharge cutoff voltage of 2.75V. However the current battery protection module cuts off all use when 2.5V is detected. This could mean the battery is overdischarged. In order to keep the battery as healthy as possible and to prevent safety hazards, it is preferable to not reach this level. Therefore the choice for the IC in Fig. 4.1 will be the R5402N205KD. This circuit prevents the battery from over(dis)charging, prevents short circuits and excess drain currents [29][26].

4.4. Battery Charger

In section 3.4 multiple chargers were discussed. To sum it up:

1. **Linear:** Requires few external components, but inefficient.
2. **Switching:** Requires many external components, but very efficient.
3. **Pulse:** Requires few external components and is efficient, but requires a current limited power source.

Since available area is limited, the switching charger is the least viable option. Additionally the pulse mode charger may not require many external components, but when charged via USB, which can deliver up to 2A, some form of current limiter is required. This basically means more components and extra cost. Even though the linear charger isn't as efficient, it's the charger that requires the least external components with the lowest cost. Therefore the linear charger was chosen.

In search of a charger, a few things were taken into account: voltage regulation, charge current, amount of external components needed, price per unit, a form of indication when it's charging or when charging is done and packaging.

The value for the voltage regulation can be found by looking at the data sheets of the batteries. Both require a charging voltage of 4.2V.

The feedback module battery has a maximum charging current of 155mA, while, coincidentally, the minimum nominal capacity is 155mAh. This basically means a maximum charge current of 1C. The goniometer battery has a maximum charging rate of 300mA, where the minimum nominal capacity is 300mAh. This allows for a more specific search.

The maximum charge rate of either battery is 1C, which means a maximum charge current of 300mA. This also limits the suitable chargers.

After extensive search, the *MCP73831* from Microchip seems like the right charger for the job, both for the goniometer and the feedback module. This series has a selectable regulation voltage of 4.20V, 4.35V, 4.40 or 4.50V and a programmable charging current of 15mA to 500mA. Dependent on which model from the MCP73831 series was chosen, the preconditioning charge current can be set. The chosen model has preconditioning current of 10% of the constant current mode, a termination current of 20% of the constant current mode and a regulated output voltage of 4.20V.

It also has STAT pin with tri-state output. When there is no battery present, or the device is in shutdown mode, the pin will be in a high impedance state. When it is charging (either through preconditioning current, constant current or constant voltage mode), the pin will be low. When the charging is complete and the device is placed in standby, the pin will be high. This allows for a charging indication, or an indication for a fully charged battery.

Then finally the packaging; this charger has an SOT-23 packaging, which allows for soldering and thus for prototyping.

The charger was implemented as seen in Fig. 4.2.

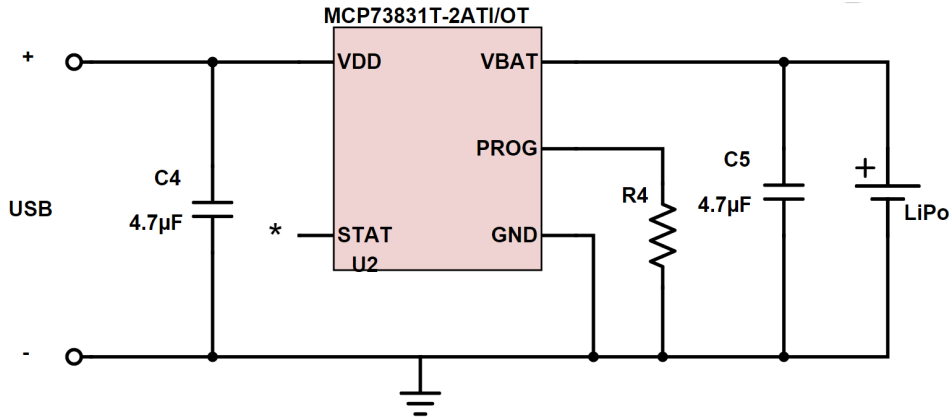


Figure 4.2: The designed charger circuit

As can be seen from Fig. 4.2, resistor R4 does not have a value. This is because the resistor connecting PROG to GND sets the constant current mode current value. Because two different absolute 1C charge rates need to be employed, two different resistor values will be needed. For the goniometer 1C charge rate means charging with $300mA$. For the feedback module this means charging with $155mA$. The value of this resistor can be found using equation 4.1.

$$R4 = \frac{1000[V]}{I_{charge}[A]} \quad (4.1)$$

Where R4 is in $[\Omega]$. This yields a resistor value for the feedback module of $6.45k\Omega$ and for the goniometer a value of $3.33k\Omega$.

An asterisk is seen at the STAT pin. This pin is optional and can be used as an indication for charging or full battery, for instance, from VDD to STAT a resistor in series with an LED could be connected. This LED would then light up as the battery is charging and turn off when it is not charging, or the battery is fully charged. This function was not implemented however.

C4 and C5 are decoupling capacitors [30].

4.4.1. Power Path Management

As was mentioned in section 4.4.1, charging and using at the same time could in some cases be problematic. Therefore the scheme in Fig. 4.3 was designed.

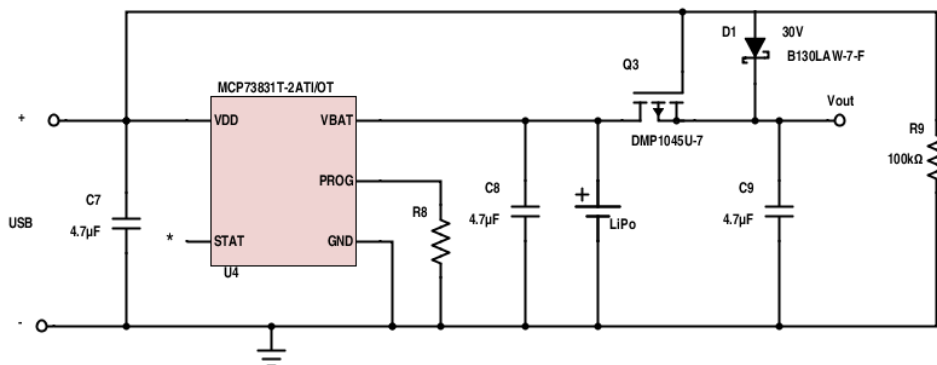


Figure 4.3: The designed power pathing circuit

When comparing Fig. 4.2 and Fig. 4.3, one can easily see that four new components have been added in 4.3, namely Q3, D1, R9 and C9.

The explanation behind these four components is rather straightforward. Q3 is a P-Channel MOSFET. Its gate is connected to the charger's positive pin. This will disconnect the battery from the load when USB is connected. Because when the USB is attached, V_{GS} will be $5 - 3 = 2V$ when the battery is fully drained or $5 - 4.2 = 0.8V$ when the battery is fully charged. This particular MOSFET has a $V_{GS,th}$ of $-0.55V$. The load will then use the power from USB. In order to reduce power losses when using the battery $R_{DS,on}$ should be as small as possible. For this particular MOSFET, $R_{DS,on}$ will have a maximum value of $45m\Omega$ [31].

D1 is a schottky diode which prevents current from flowing from the battery into the power source. The lower the forward voltage drop the better, in regards to lesser power consumption. The chosen schottky diode has a forward voltage of $0.35V$.

Then resistor R9: a pull down resistor. Its purpose is to make sure Q3 turns on and connects the battery to the load when the power from USB is removed. A value not too low should be chosen to reduce power loss. For example, a value of $100k\Omega$ will only consume $50\mu A$ [32].

4.5. Buck-Boost DC/DC converter

Because it is desired to use the battery when the battery voltage is below $3.3V$, a converter capable of boosting is needed and since the motor may use up to $220mA$ according to the data sheet [33], the inductor-based buck-boost converter was chosen as the best option. To simplify implementation and achieve cheaper bulk prices, the same converter will be used for the Goniometer and the feedback module. When searching for a buck-boost converter, the following search criteria was used to try and find the most suitable component:

1. Use as less external component as possible to reduce the board area consumed.
2. Be able to have a peak output current equal to the summation of the peak current of the motor and the rest of the feedback module's components. This is approximately $550mA$.
3. An efficiency of about 90% under a load between $60mA$ and $170mA$, which are the nominal currents of the Goniometer and the feedback module.

The amount of available converters is very extensive and finding a suitable component proved to be time consuming, partly due to inexperience with searching parts. A suitable candidate was found to be the TPS63024, but unfortunately this IC was only available in the DSBGA package, which was advised by the supervisor to not be suitable for prototyping and production, and an evaluation kit is expensive (50 USD). This added another search criteria: a packaging which was more suitable for prototyping. Searching revealed the LTC3440 to be suitable.

This converter can have an efficiency of above 90% for output currents between $10mA$ and $200mA$. At very low load currents, such as when the powered device is in standby, switching regulators usually have a very low efficiency, but Linear Technologies has implemented the burst mode for this situation. In this mode the efficiency can be up to 79% for load currents below $30mA$, according to the data sheet. Using the typical application circuit as a lead, the circuit depicted in figure 4.4 has been designed.

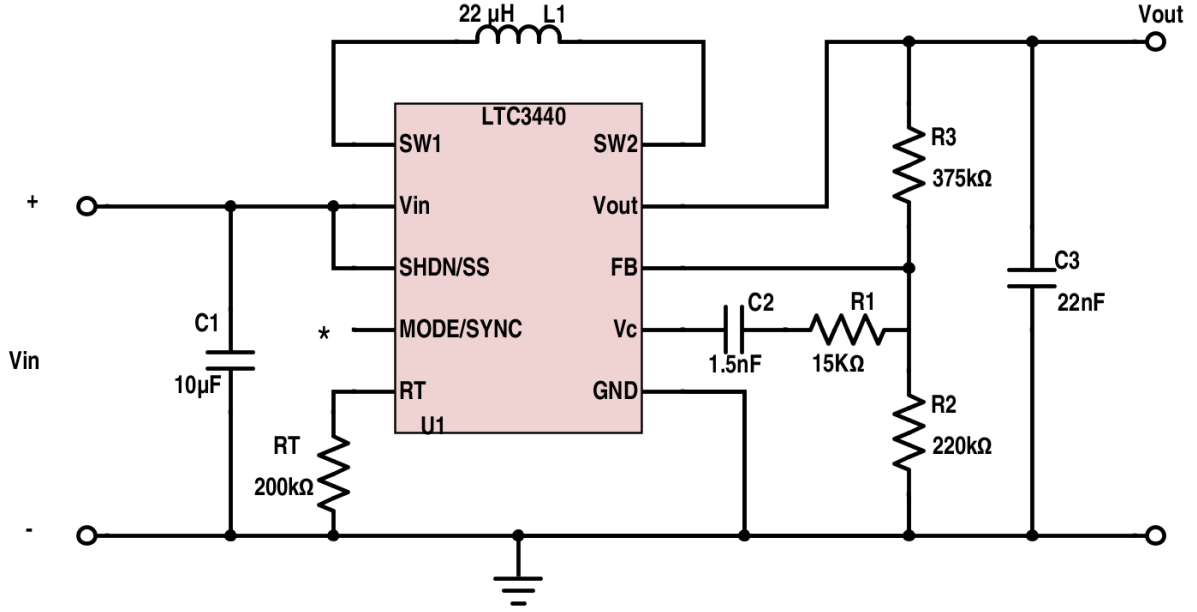


Figure 4.4: The designed buck-boost circuit

The 10-MSOP package was chosen. The MODE/SYNC pin can be pulled high for burst mode operation and pulled low for fixed frequency operation. The difference between these two modes is the efficiency at different loads. Fixed frequency is more efficient for loads starting at about 5mA and burst mode below that. When the device is in standby, burst mode should be used, otherwise fixed frequency. This can be implemented with a switch controlled by the microprocessor. The next step is to choose the resistor R3 and R2. These resistors program the output voltage. The voltage at the FB port is regulated to be 1.22V, and due to C2 forming an open circuit in steady state, the output voltage[V] is described by the voltage division between R2[Ω] and R3[Ω]:

$$V_{out} = \frac{1.22}{R2} (R2 + R3) \quad (4.2)$$

The value of 220kΩ for R2 is derived from the order of magnitude in the typical application description in the data sheet. R3 can then be calculated by rewriting equation 4.2 and substituting the values to find 375kΩ.

The operating frequency can be selected with timing resistor R_T . The operating frequency is chosen to be 300kHz, since this is the lowest possible frequency this will result in the highest efficiency since the losses due to gate charge are proportional with the frequency. The drawback of choosing a lower frequency is the increase in capacitor and inductor size. Because BLE transmits at 2.4GHz, the RF noise created by the circuit will not interfere at this frequency. Following the simple equation given in the data sheet results in a value of 200kΩ.

The next step is to choose the inductor value. According to the data sheet, there are two equations that determine the minimum value for the inductor[μH]:

$$L > \frac{V_{In(min)} * (V_{out} - V_{In(min)})}{f * I_{out(max)} * Ripple * V_{out}} \quad (4.3)$$

$$L > \frac{V_{out} * (V_{In(max)} - V_{out})}{f * I_{out(max)} * Ripple * V_{In(max)}} \quad (4.4)$$

Where f [MHz] is the operating frequency, $V_{In(min)}$ [V] the minimum input voltage, $V_{In(max)}$ [V] the maximum input voltage, V_{out} [V] the output voltage, $I_{out(max)}$ [A] the maximum output load current and *Ripple* the inductor current ripple, which is typically set between 20% and 40%. The largest value produced by these equations thus sets the minimum. The ripple is chosen to be low, so 20%. Substituting the values produces an inductance of 21.4μH.

After building the circuit it was tested with a 62Ω load. In burst mode this gave an efficiency of 73% and an output voltage of 3.3V. However, in fixed frequency mode the efficiency was only 19%, which is far below the expected value of 95%. It is not exactly clear why the fixed frequency mode does not work. One possible clarification would be the layout of the circuit. The inductor should be placed as close as possible to the chip and for this a PCB had to be designed, which there wasn't enough time for.

4.6. Battery Gauge

Monitoring a battery is not an easy task as was explained in section 3.5. When looking for the proper battery gauge, a couple of aspects were taken into account, namely the price, how many cells could be monitored, what kind of chemistry it could monitor and lastly again, the package. A couple of different methods were mentioned in section 3.5. The decision has fallen on the DS2782 from Maxim Integrated Products. This is a 2-wire stand-alone fuel-gauge IC capable of calculating the remaining battery capacity in *mAh* or percentage of full for Li-Ion or LiPo single cell batteries. This particular battery gauge uses a regular coulomb counter, however, by fully draining the battery once in approximately 3 months and then allowing it to recharge to full, the accumulated current error can be eliminated. The regular coulomb counter was chosen because the other methods mentioned in section 3.5 are patented so the GonioTrainer would be dependent on one particular manufacturer, whereas this was to be avoided if possible. The package is TSSOP which allows for soldering by hand. The designed circuit can be seen in Fig. 4.5. As can be seen, some additional components are needed.

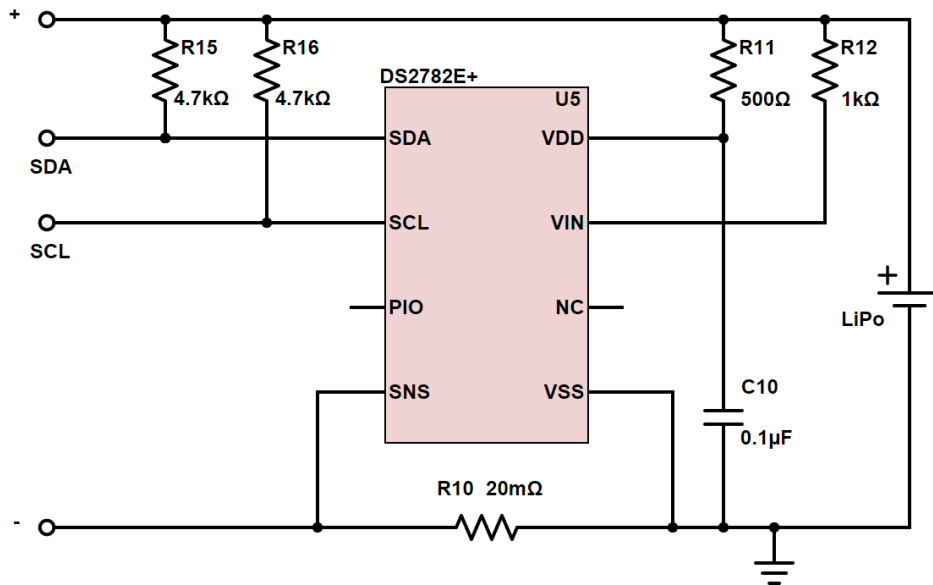


Figure 4.5: The designed battery fuel gauge circuit

The PIO pin can be configured as an input or output to monitor or control external user-defined external circuitry. This was not used. The NC pin means No Connection, which is what was done. One might think a lot of external components were required, but 2 of them were necessary for I²C. Resistors R15 and R16 are pull up resistors. Resistor R11 and capacitor C10 form a decoupling network and the values for these components are taken from the typical operating circuit found in the datasheet. R12 is a typical 1kΩ resistor act as a voltage divider with the input impedance of V_{IN} , which is $15M\Omega$. In order to account for the accumulated errors mentioned earlier, the gauge contained registers used to eliminate this error. This was done using I²C.

After writing these values to non-volatile EEPROM, these settings are kept even if the gauge loses power. The total accumulated current will be stored every time the battery is fully charged and the gauge sets a flag [34].

4.7. Vibration Motor

In this section the implementation of the actuator on the feedback module will be discussed. The selection of the ERM motor will be followed by the implementation of the driver and adjustable settings.

4.7.1. ERM motor

Two options for the ERM motor were given: the Pico Vibe 9mm vibration motor and the Precision Haptic 8 mm vibration motor. These motors will be compared on the following characteristics:

1. Power consumption. Lower power consumption has a preference.
2. Rise time and lag time. A lower start up time decrease the total lag time from feedback moment detection to observable feedback.
3. Possible vibration amplitudes within the supply voltage range, thus up to 3.3V.
4. Active braking time at maximum reverse voltage. Active braking time should be lower than 35ms for pulsing mode.

Table 4.2: Comparison table for the ERM motors

	Power consumption[mWh]	Rise + lag time [ms]	Typical active brake time	Vibration amplitude [g]
Pico Vibe 9mm	99	36	21	0.2-8.0
Precision Haptic 8mm	145	30	20	0.2-3.6

The power consumption is the worst case scenario as was calculated in section 3.2.1. The rise, lag, braking time and vibration amplitude is derived from the data sheet of the motors. The client advised that the motor should give an amplitude of at least 5g. This makes the Precision Haptic an unsuitable option. The Pico Vibe has characteristics which are in accordance with the previously mentioned criteria, thus it will be selected as the actuator.

4.7.2. Motor driver

To drive the motor two options were considered, the PWM controlled MOSFET switch, or a dedicated IC. According to the data sheet of the Pico Vibe, the typical stop time is 49ms and since the inter burst duration should be 35ms, active braking should be implemented. Because active braking with the MOSFET controlled switch might be complex, since there should be feedback on the speed of the motor to only brake and not reverse, the dedicated IC option has been chosen.

The following search criteria were followed when searching for a suitable driver:

1. Output driving voltage up to 3.3V to be able to drive the motor to what is maximally possible with the output voltage of the buck-boost converter.
2. Digital control input. The control signal will come from the nRF51822 and since neither the nRF51822 or the ISP130301 has an onboard DAC, it is preferred to have a digital input to control the motor.
3. Suitable package for prototyping.

Searching produced the DRV2605L to be a suitable candidate. This driver is specifically designed for linear resonance actuators and ERM's. The 10-pin VSSOP package was used. It has a feedback architecture based on the back EMF, which is used for automatic braking and over driving, see appendix B.1 for an overview of the architecture. Furthermore the external control signal can be selected via I²C to be PWM. The designed schematic, derived from the typical application for PWM mode described in the data sheet [35], can be seen in figure 4.6.

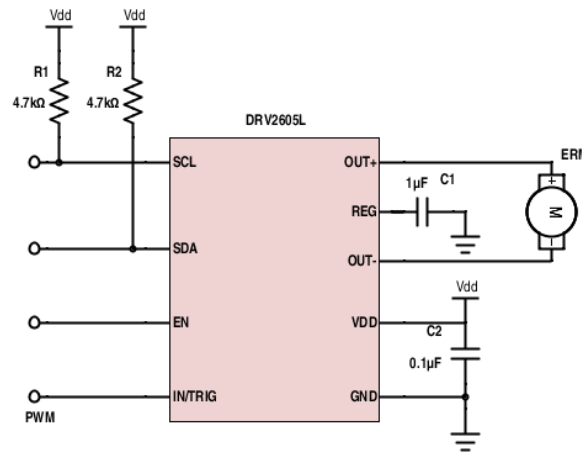


Figure 4.6: The designed driver circuit

R1 and R2 function as pull-up resistors. The value is based on the maximum value recommended in the data sheet to reduce power consumption. C1 and C2 are low equivalent series resistance (ESR) bypass capacitor needed for proper operation.

This driver does have to be calibrated and a series of registers have to be set via I²C. Certain parameter registers are a result of the auto calibration process. These registers hold the information for the following purposes:

1. A voltage compensation for any resistive losses in the driver.
2. The back EMF when the motor is driven at the maximum voltage. The driver uses this value to automatically determine the appropriate feedback gain.
3. The analog gain of the back EMF amplifier.

The original plan was to let the driver perform the calibration upon subsequent power ups to adjust to changes in the motor over the course of time, but the auto calibration procedure failed many times or did not produce suitable results during testing. The calibration procedure succeeded when the supply voltage was 5V, but never with 3.3V. This was odd since the maximum overdrive voltage was sometimes set to less than 3.3V. The results of the auto calibration with a supply voltage of 5V produced satisfactory results when the supply voltage was 3.3V, so these settings will be hard coded in the initialisation function of the code. The results of the auto calibration can be written to the one time programmable memory (OTP) of the registers described above, which is nonvolatile memory and thus the auto calibration process does not have to be run on each start up. Because this project is in the prototyping phase, this memory will not be used but could be useful when the product is in production. Furthermore the DRV2605L has a library with waveforms that could be played, but many parameters of these waveforms can not be set and there was not enough time for testing these, but it could be useful.

4.7.3. Adjustable settings

The magnitude of the steady state output voltage of the driver can be adjusted linearly with the duty cycle of the PWM input. See appendix B.2. Based on the performance graph of the Pico Vibe, see appendix B.3 it can be approximated that the vibration amplitude increases linearly with the input voltage starting at 1V. So the vibration amplitude will be approximately proportional to the duty cycle of the PWM signal. This diminishes the need for a look up table to linearly adjust the vibration amplitude based on the user defined settings.

The next step is to define the settings and how this information will be formatted. The user defined settings will be the vibration amplitude, length of vibration and pulsing or constant vibration. Other settings, such as the pulse mode parameters, can be changed in the code. All the user defined settings along with the command to run the motor will be contained in one byte sent from the smart phone.

4.8. Final Design

In this section the final design will be portrayed. In Fig. 4.7, the final block schematic of design treated in this thesis can be seen. The entire schematic, all components included can be seen in Appendix C, section C.1.

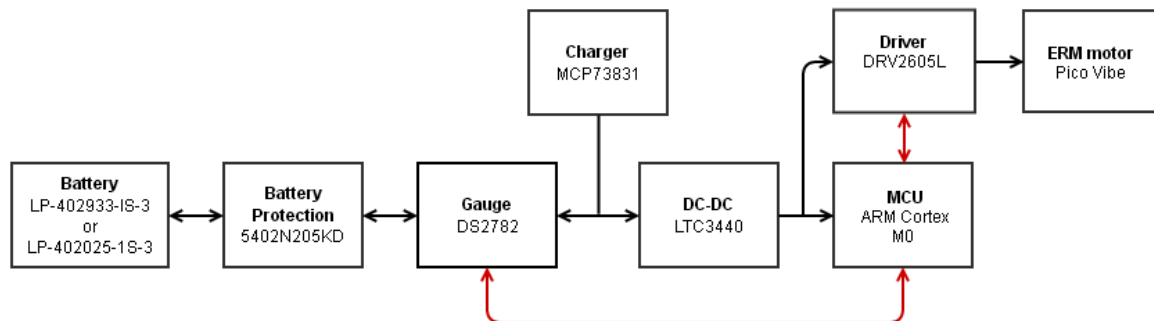


Figure 4.7: Block schematic of the system. Black arrows indicate power flow and red arrows indicate data transfer

5

Results

5.1. Battery Protection, Battery Charging, Power Path Management & Battery Gauge

Charging a battery and protecting it from overcharging go hand in hand. As mentioned numerous times, overcharging a battery can be dangerous and overdischarging can damage the battery's capacity and can be dangerous when charged subsequently. However, in order to test our protection circuit, this is exactly what was needed. Overcharging a LiPo battery can be an immediate safety hazard, therefore it was decided to not test this. Moreover the designed charger circuit should not even allow this. It was decided to not test this but to assume, after studying the protection circuit, that this would work.

The charging process was tested using the circuit depicted in Fig. 4.3. The result can be seen in Fig. 5.1. A load of 62Ω was applied to the circuit. As was explained in section 3.4.5, when a supply voltage of $5V$ is applied, this will feed the battery charging circuit, as well as the load. A $5V$ supply with a 62Ω load will deliver an additional $5/62 = 80mA$ to the $155mA$ the charger requires. This is the value of the orange line minus the blue line, where the orange line is the current supplied by the power supply and the blue line shows the current flowing into the battery.

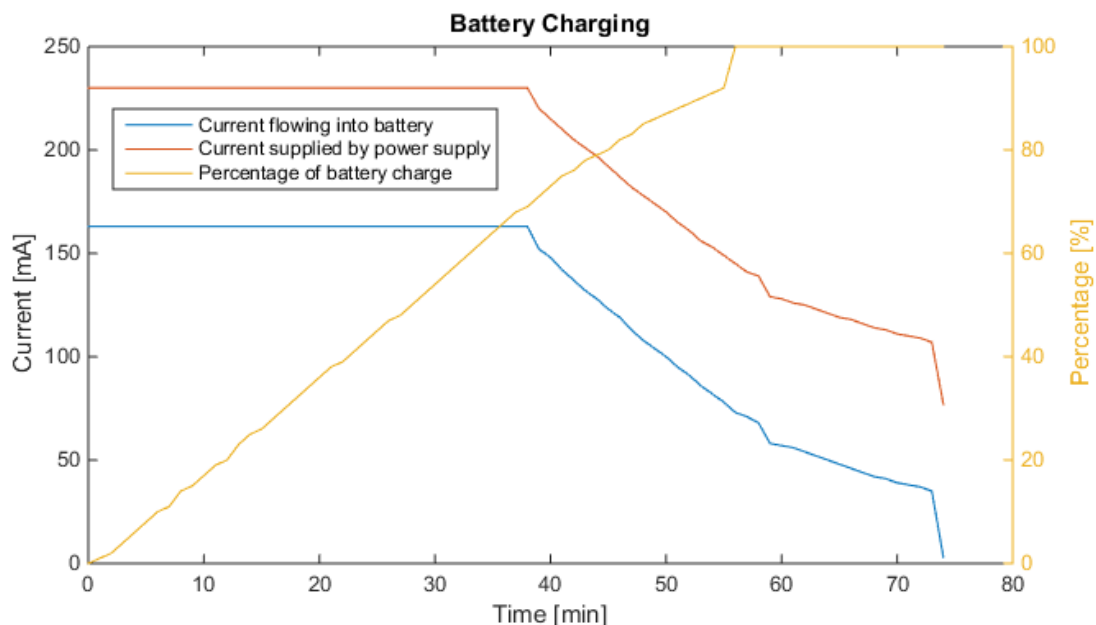


Figure 5.1: The current plotted versus time.

The x-axis of Fig. 5.1 shows the time in minutes. On the left y-axis the current in mA is shown. The

right y-axis shows charge percentage of the battery. At almost 40 minutes in, the current drops. This is not yet the point where the constant voltage mode was achieved, however the temperature of the charger IC became too high. The built in overheat protection gradually lowered the current in order to keep charging the battery, but to protect itself from overheating. This is in accordance with the duration of the total time charged. Because the charging current lowered itself, the battery wasn't being charged at 1C anymore, thus the duration would have had to increase past the 1 hour mark.

Because the current already lowered itself, it's hard to pinpoint exactly where the constant voltage mode was entered. However, it was entered, because at $30mA$, the current at which the chosen charger model would stop charging, the charger prevents current from flowing in and only the current supplied to the load remains.

Then finally the charge percentage of the battery shows to be full at approximately 55 minutes. As was mentioned in section 3.5.1, a battery gauge has an EOC value. The datasheet of the battery gauge advised to place this value marginally lower than the actual value. The entered value was probably entered slightly too low and thus the gauge thought the battery was fully charged.

5.2. Motor driver

To test the driver, the motor has been connected to the driver and the voltage at the motor terminals was measured with the oscilloscope. Unfortunately the brush component of the motor broke right before testing and there was not enough time to obtain a new one. The brushes were improvised by holding wires against the commutator. The results can be seen in figure 5.2. The voltage increases approximately linearly as expected up to the programmed rated voltage of $3.3V$. The motor noticeably increased in vibration amplitude, but there were no means for measuring the vibration amplitude with a clamped broken motor. The current does exceed the value of the data sheet, but this could be due to numerous factors influencing the mechanical load and thus a need for higher torque.

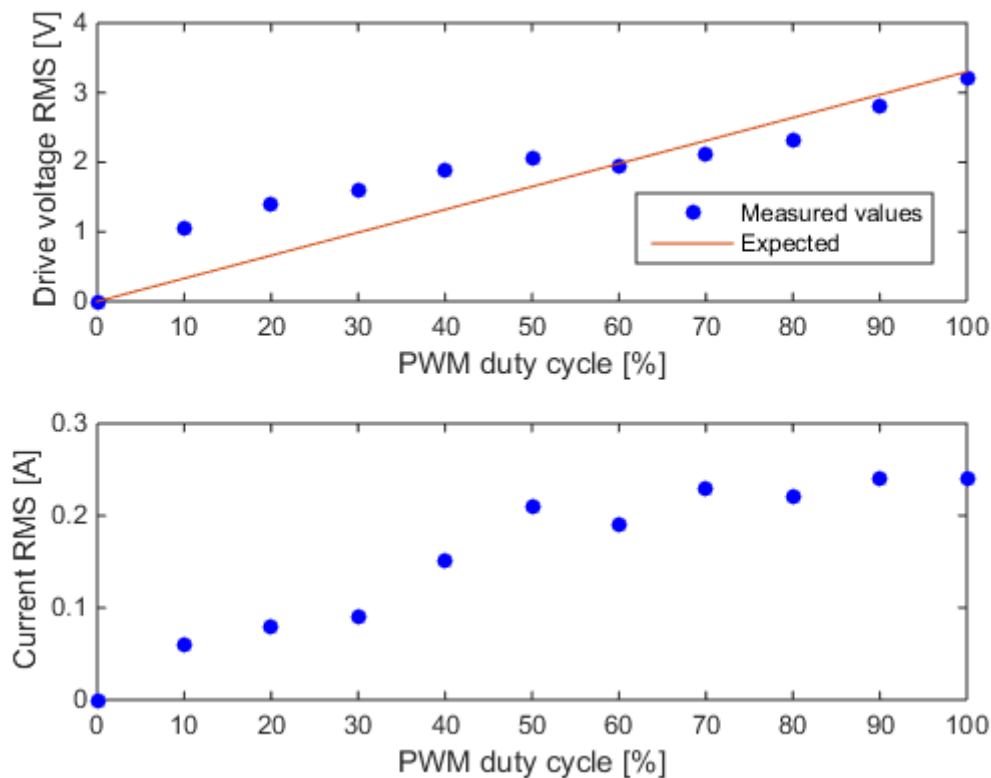


Figure 5.2: The measured results of the driver.

5.3. Feedback control via smartphone

The ability to set the vibration settings and send the command to vibrate via the smart phone was implemented and works when data is received. However the connection becomes unreliable when PWM is used. This is due to the timers interrupt not being serviced on time, but there are different PWM libraries which should work [36]. A different implementation of a provided PWM libraries were tried to no avail.

5.4. Weight and size

The maximum required dimensions have not been met, this is mostly due to the feedback motor alone being larger than the maximum dimensions. Whether the maximum weight limit has been broken or not cannot be established. The weight of the motor is 4.6g, the weight of the battery is 4g. The weight of the ISP is not listed in its datasheet. A PCB was not created thus the weight thereof could not be taken into account. All the other parts like SMD resistors, capacitors or coils will probably not sum to an amount that needs to be accounted for.

5.5. Pricing

All of the chosen components come with a price. When buying components in larger quantities, discounts apply. The component with its cost for 10 pieces and total sum can be seen in Table 5.1.

Table 5.1: A list of components and their price per unit when purchasing more than 10

Component	Quantity	Price (euro)	Amount	Subtotal	Store
Driver	10+	3,7	1,00	3,7	Farnell
Gauge	10+	5,75	2,00	11,50	Farnell
Charger	10+	0,479	2,00	0,958	Farnell
DC-DC	10+	6,92	2,00	13,84	Farnell
Bat1(300)	10+	14,9	1,00	14,9	Farnell
Bat2(165)	10+	14,39	1,00	14,39	Farnell
ISP	10+	9,8	2,00	19,6	Texim-Europe
Flash	10+	6,03	1,00	6,03	Farnell
IMU	10+	5,87	1,00	5,87	Invensense
Hoeksensor	10+	2,44	1,00	2,44	Mouser
Motor	10+	6,77	1,00	6,77	Precision Microdrives
Total 10+:				99,998	

The prices and the sum when buying 100 pieces are displayed in Table 5.2.

Table 5.2: A list of components and their price per unit when purchasing more than 100

Component	Quantity	Price (euro)	Amount	Subtotal	Store
Driver	100+	2,53	1,00	2,53	Farnell
Gauge	100+	5,00	2,00	10,00	Farnell
Charger	100+	0,396	2,00	0,792	Farnell
DC-DC	100+	3,56	2,00	7,12	Farnell
Bat1(300)	100+	10,79	1,00	10,79	Farnell
Bat2(165)	100+	9,8	1,00	9,8	Farnell
ISP	100+	8,33	2,00	16,66	Texim-Europe
Flash	100+	5,42	1,00	5,42	Farnell
IMU	100+	5,59	1,00	5,59	Invensense
Hoeksensor	100+	2,01	1,00	2,01	Mouser
Motor	100+	6,3	1,00	6,3	Precision Microdrives
Total 100+				77,012	

Neither Table 5.1, nor Table 5.2, have taken small components like resistors, capacitors or coils into account.

As can be seen from Table 5.1, one unit worth of electronics will cost €99.998. When looking at the specifications, a unit's electronic could cost a maximum of €60, with a total cost of €100. This is 60% of the maximum cost. When taking this 60% of €2500, a unit's electronic would have a maximum value of €150. This has been accomplished.

Applying this same logic to the price specification of buying a 100 units, a unit's electronic could have a maximum value of €60. Unfortunately, this limit has been exceeded by €17.012.

6

Discussion

After acquiring more knowledge in this field and reviewing the system as a whole, thoughts of a better implementation arise. These thoughts will be discussed in this section.

6.1. Use of buck converter

Only a slight portion of a LiPo battery's capacity is stored below the $3.3V$ level. In this view it may be better to consider the battery to be empty at $3.3V$, instead of boosting the remaining capacity which may not extend the time of use that much. Buck converters are usually cheaper and can lower the cost of the product.

6.2. Driver directly connected to the battery

The chosen driver can supply a constant drive output over variation of the supply voltage, so there is no need for a constant voltage. However, the driver can not boost the input supply voltage. Limiting the battery discharge level to $3V$ with the protection circuit guarantees that lowest operational supply voltage will be $3V$ and thus the maximum output can be set to this voltage level. The loss in maximum vibration amplitude from $3.3V$ to $3V$ will be $7.75 - 7.0 = 0.75g$. The advantage of this is that there will be no power loss in the voltage converter since the current will flow directly to the driver.

7

Ethics

In this day and age, technology is developing at a rapid pace. Technology's advancements have gone so quickly, engineers can easily overlook the ethical aspect. Just because something can be build, does not mean it has to be. Before one starts to develop a device/application/drug, one should ask themselves the question: "If I develop X, would that be ethically justifiable?"

7.1. Consequentialism

Utilitarianism is the most known form of consequentialism. From the utilitarianism point of view, one acts to maximize utility. However, utility can mean a lot of things, for instance happiness, economical well being or no suffering. Jeremy Bentham, one of the most influential person of utilitarianism defined it as: "it is the greatest happiness of the greatest number that is the measure of right and wrong". When looking at the use of the GonioTrainer from a utilitarians point of view, one could argue that, because of the price of the GonioTrainer, not every athlete would be able to buy this and thus these people would not receive happiness when other athletes with the GonioTrainer achieve better results. However, the stakeholders of the GonioTrainer would in turn receive happiness because their product sold and they made money. Two different meanings of the word happiness have been used here. Is the one better than the other? Say for instance the happiness of the athletes is worth more than the happiness of the stakeholders. Who would decide this?

Another aspect to look at would be the safety of the GonioTrainer. As the GonioTrainer was developed, a certain type of battery was chosen. Batteries do not come without risks. Should one blow up, even though multiple precautions were taken, nobody involved with the GonioTrainer would receive happiness. Least of all the person using the device that blew up. Would this aspect, which could be the fault of the user and not the engineer, not make the GonioTrainer ethically justifiable?

7.2. Virtue Ethics

Virtues have always been around, however they have undergone changes throughout the years. In virtue ethics there is emphasis on how people practice virtues. When looking at the GonioTrainer through virtue ethics in modern day society, a virtue, or value, could be performance, because people are pushing records to the limit in sports. However without the aid of technology and modern day measurement systems, these limits would never be broken. Therefore people who would use the GonioTrainer in order to set new records, would be able to justify the use of the GonioTrainer from the perspective of virtue ethics.

7.3. Deontological ethics

Deontological ethics looks at one's intentions rather than the outcome. The company behind the GonioTrainer has a first and foremost intention of making money, which, in itself, isn't wrong. It's how they go about this. They want to deliver a grade A quality product which will actually aid the users in their intention of improving performance. Their second intention is to aid the users. Their intentions

are good.

Users will use the GonioTrainer in order to improve performance in sports. Their intention is improving. There is no harm in that. That others may not be able to improve because they cannot afford the GonioTrainer is not something deontological ethics takes into account. Therefore both the users and the company ethically justify the use and creation of the GonioTrainer.

7.4. Philosophy of dialogue

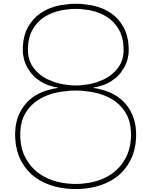
People tend to stick to their routines. Everyone has their own perception of the world around them. We live by this perception and act accordingly. Naive and satisfied we stay in this known perception, as if we're walking in circles. Levinas called this: "Self". However, the interaction with another human being intrudes this Self. We are forced to answer to this other person's calling. We cannot force this other, and therefore might write it with a capital too: "Other". In regard to the GonioTrainer, it's a new development and will have to answer to the users. Only the company/engineers behind the GonioTrainer can answer the calling and questioning of the users. However not every answer should be newly forged, some values of modern day society and juristic laws are to be followed. The company/engineers will of course try to create a product that will adhere to these standards and will be able to ethically justify their new development from the perspective of the philosophy of dialogue.

7.5. Conclusion

From three out of the four mentioned ethical point of views, the use and development of the GonioTrainer is ethically justifiable. Moreover, one cannot stop technological advancement. This particular product can cause very little damage when used improperly, when compared to a car, which can actually kill multiple people.

To keep the car comparison going, the GonioTrainer uses less power than a car and has less parts that should be treated carefully when being disposed. If a car is ethically justifiable, why wouldn't the GonioTrainer?

We are therefore inclined to say that the creation and the use of the GonioTrainer is ethically justifiable.



Conclusion

The entire project was split up into three sub-projects. The group that wrote this thesis was assigned to the power supply, which entails making sure that all components are supplied with sufficient power at the right voltage and giving information about the battery's status. Furthermore they will design the feedback module, but excluding the communication link and peak detection algorithm.

The power consumption of both the feedback module and the goniometer have been calculated and will be able to be supplied with power for a 3 hour usage session. A battery protection circuit that will protect the battery from overcharging, overdischarging and over current has been designed and integrated. The charger was able to charge the battery from fully drained to fully charged. While a power supply was connected to the charger, the power supply would also feed the load and charge the battery at a 1C current. The battery gauge was able to determine the percentage of the battery accurately and will continue to improve its accuracy as more charge cycles are completed.

The feedback module will be able to give haptic feedback either in pulses or continuous mode. The pulse length wasn't measured accurately, thus the required of 65ms pulses and 35ms pauses were not tested. The amplitude of vibration can be set in approximately linear steps.

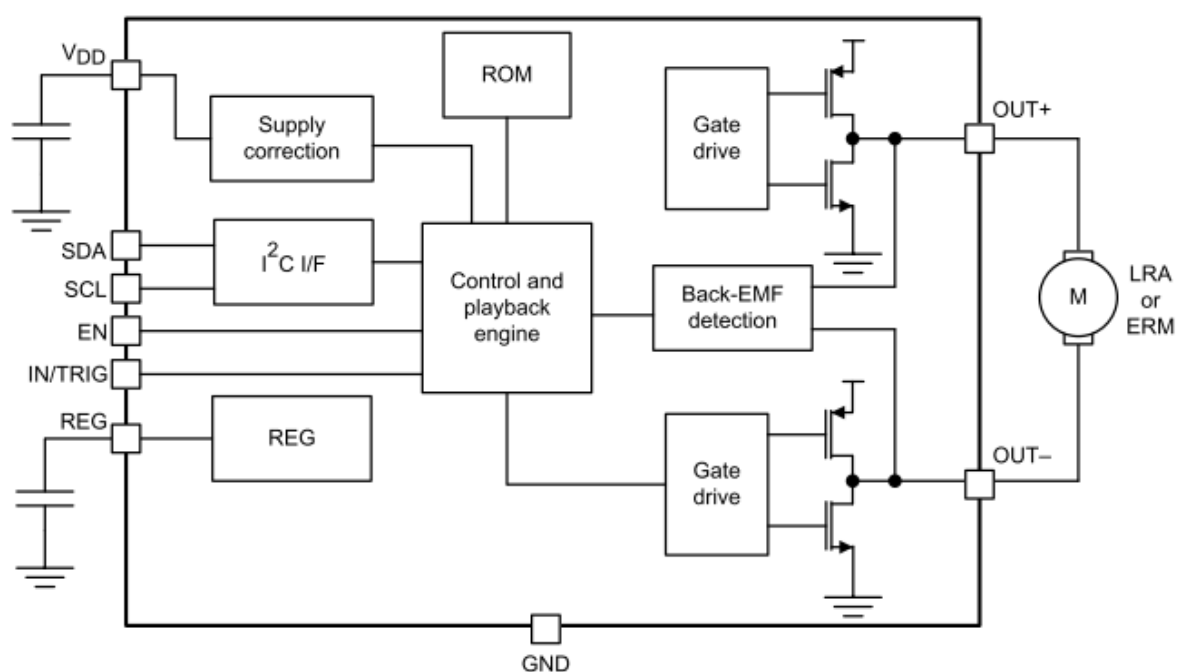
The integration with bluetooth, however, was not successful neither was the buck-boost converter.

[illegible]

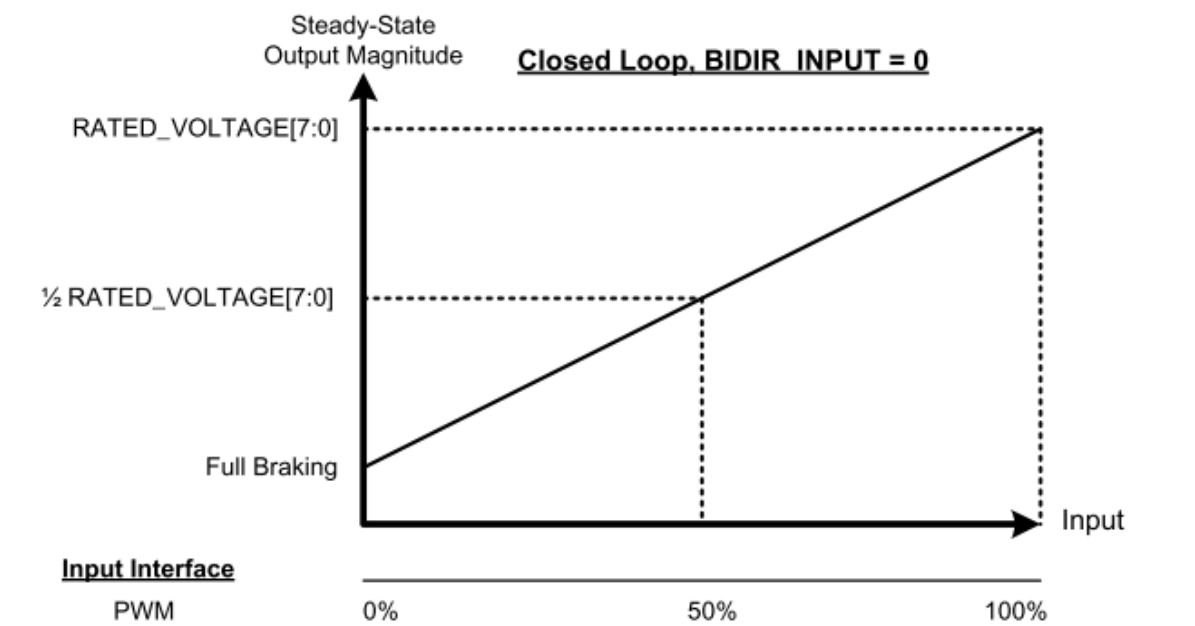
B

DRV2605L

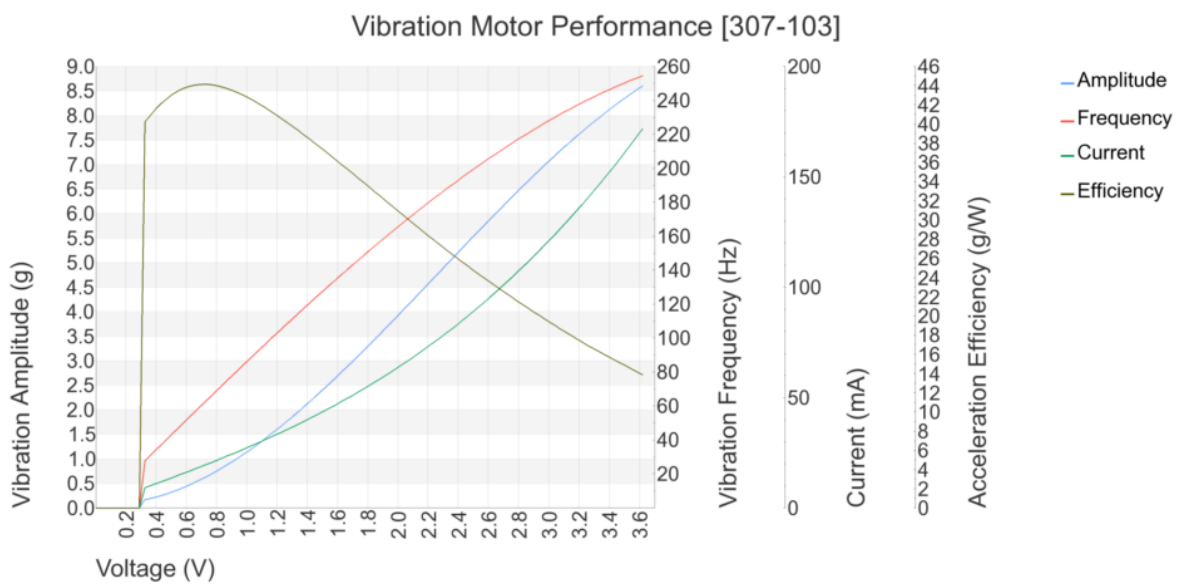
B.1. Block diagram

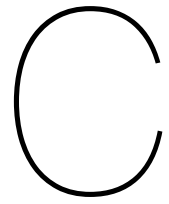


B.2. Output-input graph



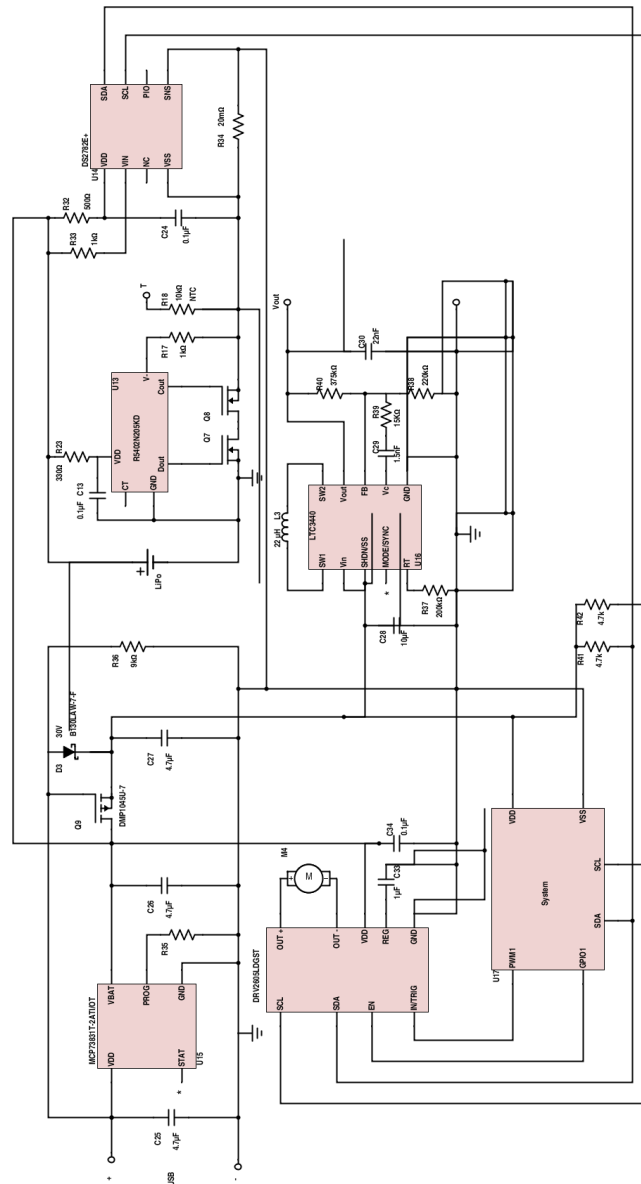
B.3. Pico Vibe performance graph





Total Design

C.1. Schematic



Bibliography

- [1] K Townsend, C Cufí, and R Davidson. *Getting Started with Bluetooth Low Energy: Tools and Techniques for Low-Power Networking*. ISBN 9781491949511.
- [2] Apple Inc. Bluetooth Accessory Design Guidelines for Apple Products. *History*, page 22, 2011.
- [3] Nordic employee. 51822 bluetooth, November .
- [4] AMS. AS5601 12-bit Programmable Contactless Encoder. page 5, 2014.
- [5] InvenSense. MPU-6000 and MPU-6050 Product Specification. 1:14, 2013.
- [6] Nordic Semiconductor. nRF51822 specifications. (November), 2008.
- [7] Precision Microdrives. Precision Haptic™ Model : 308-102. pages 1–7, 2013.
- [8] David Linden and Thomas B Reddy. *Handbook of Batteries*. 2001. ISBN 0071359788. doi: 10.1016/0378-7753(86)80059-3.
- [9] Battery University. Bu-301a: Types of battery cells. http://batteryuniversity.com/learn/article/types_of_battery_cells.
- [10] Walter A. Schalkwijk Van and Bruno Scrosatie. *Advances in Lithium-Ion Batteries*. KLUWER ACADEMIC PUBLISHERS, 2002. ISBN 0306475081.
- [11] Woodbank Communications Ltd. Lithium battery failures. http://www.mpoweruk.com/lithium_failures.htm, 2005.
- [12] Hossein Maleki and Jason N. Howard. Effects of overdischarge on performance and thermal stability of a Li-ion cell. *Journal of Power Sources*, 160(2 SPEC. ISS.):1395–1402, 2006. ISSN 03787753. doi: 10.1016/j.jpowsour.2006.03.043.
- [13] Steven Keeping. A designer's guide to lithium battery charging. Technical report, Electronic Products, sep 2012.
- [14] C Hapter and a Jossen. Battery Management. page 10, 2004.
- [15] Maxim Integrated Products. Switch-Mode, Linear, and Pulse Charging Techniques for Li + Battery in Mobile Phones and PDAs. *Maxim Application Notes*, pages 1–6, 2001.
- [16] Universal Serial Bus Specification. *Group*, page 178, 2000. URL http://www.usb.org/developers/docs/usb_20_071411.zip.
- [17] Battery University. http://batteryuniversity.com/learn/article/inner_workings_of_a_smart_battery, May 2015.
- [18] Vincent Ho. Li-ion Battery and Gauge Introduction. pages 6–10, September 2014.
- [19] Maxim Integrated Products. ModelGauge m3 Fuel Gauge MAX17047 / MAX17050 ModelGauge m3 Fuel Gauge. pages 9–10, 2014.
- [20] Henry J Zhang. Application Note 140 October 2013 Basic Concepts of Linear Regulator and Switching Mode Power Supplies AN140-1 Application Note 140 AN140-2. (October):1–16, 2013.
- [21] Maxim Integrated. Choosing the Right Power-Supply IC for your Application. 2014. URL <http://www.maximintegrated.com/app-notes/index.mvp/id/737>.

- [22] Ab-004:understanding erm vibration motor characteristics. <http://www.precisionmicrodrives.com/application-notes-technical-guides/application-bulletins/ab-004-understanding-erm-characteristics-for-vibration-applic>
- [23] Ab-001: Discrete driver circuits for vibration motors. <http://www.precisionmicrodrives.com/application-notes-technical-guides/application-bulletins/ab-001-discrete-driver-circuits-for-vibration-motors>.
- [24] G.J. van Raamsdonk E.R.A. Visser. Bachelor thesis GonioTrainer. 2014.
- [25] https://developer.mbed.org/media/uploads/chris/mbedqa_v1.0.pdf.
- [26] Specification of Li-polymer Rechargeable Battery, LP-402933-1S-3. 2012.
- [27] Specification of Li-polymer Rechargeable Battery, LP-402025-1S-3. 2012.
- [28] ShotTracker. Shottracker devices. <http://shottracker.com/devices/>.
- [29] R5402N163KD-TR-F, Product Specifications. pages 1–11.
- [30] Microchip. MCP73831/2 (Datasheet). pages 1–28, 2014.
- [31] Diodes Incorporated. DMP1045U P-CHANNEL ENHANCEMENT MODE MOSFET (Datasheet). pages 1–6, April 2015.
- [32] Brian Chu. Designing A Li-Ion Battery Charger and Load Sharing System With Microchip's Stand-Alone Li-Ion Battery Charge Management Controller. pages 1–10, 2008.
- [33] Linear Technology Corporation. LTC3440 - Micropower Synchronous Buck-Boost DC/DC Converter. pages 1–20.
- [34] Maxim Integrated Products. DS2780 Standalone Fuel Gauge IC. pages 1–31.
- [35] DRV2605L 2 to 5.2 V Haptic Driver for LRA and ERM With Effect Library and Smart-Loop Architecture. 2014.
- [36] Tuze Kuyucu. <https://developer.mbed.org/questions/3733/When-I-use-the-BLE-functionPWM-is-not-su/>, 2014.